Bacterial communities adapted to higher external resistance can reduce the onset potential of anode in microbial fuel cells

Bacterial communities adapted to higher external resistance can reduce the onset potential of anode in microbial fuel cell

Kei Suzuki[1], Yutaka Kato[2], Arashi Yui[2], Shuji Yamamoto[2], Syota Ando[2], Owen Rubaba[3], Yosuke Tashiro[2] and Hiroyuki Futamata[1,2,4]*

[1]*Graduate school of Science and Technology, Shizuoka University, Hamamatsu, Hamamatsu 432-8561, Japan*; [2]*Department of Applied Chemistry and Biochemical Engineering, Graduate School of Engineering, Shizuoka University, Hamamatsu, 432-8561, Japan, and* [3]*College of Health Sciences, University of KwaZulu-Natal, Durban, 4000, South Africa*; *and* [4]*Research Institute of Green Science and Technology, Shizuoka University, Suruga-ku, Shizuoka, Shizuoka 422-8529, Japan*

Short title: Adaptation to external resistance

Key words: Microbial fuel cell; External resistance; Adaptation of Microbial community; Extracellular electron transfer; Onset potential

*Corresponding author.
Mailing address: Department of Applied Chemistry and Biological Engineering, Graduate School of Engineering, Shizuoka University, Hamamatsu, 432-8561, Japan
Phone: +81-53-478-1178
Fax: +81-53-476-0095
e-mail: futamata.hiroyuki@shizuoka.ac.jp

Abstract

We investigated how bacterial communities adapted to external resistances and exhibited the performance of electricity production in microbial fuel cells (MFCs) with external resistance of 10 Ω (LR-MFC) and 1000 Ω (HR-MFC). The HR-MFC exhibited better performance than the LR-MFC. The power densities of the LR-MFC and the HR-MFC were 5.2±1.6 mW m^{-2} and 28±9.6 mW m^{-2} after day 197, respectively. Low-scan cyclic voltammetry analyses indicated that the onset potential of the HR-MFC was more negative than that of the LR-MFC, suggesting that the higher external resistance led to enrichment of the highly current producing bacteria on the anode surface. All clones of *Geobacter* retrieved from the LR-MFC and the HR-MFC were members of the *G. metallireducens* clade. Although the population density of *Geobacter* decreased from days 366 to 427 in the HR-MFC, the current density was almost maintained. Multidimensional scaling analyses based on denaturing gradient gel electrophoresis profiles indicated that the dynamics of the biofilm and anolytic communities changed synchronously in the two MFCs, but the dynamics of the bacterial communities in the LR-MFC and the HR-MFC were different from each other, reflecting different processes in adaptation to the different external resistances. The results suggest that the microbial community structure was formed by adapting to higher external resistance, exhibiting more negative onset potential and higher performance of the HR-MFC through collaborating with anode-respiring bacteria and fermenters.

Introduction

Chemical and biological approaches to sustainable energy production, such as using methane, ethanol, and hydrogen, have been developed. However, many of these approaches have encountered technical and economical hurdles (1, 2). Microbial fuel cells (MFCs) represent an alternative strategy capable of directly converting organic waste to electricity (3, 4). MFCs are devices that exploit numerous and diverse microorganisms as "biocatalysts" to generate electric power from organic waste such as wastewater and garbage. It is important for the practical application of MFCs to improve harnessing structure, including electrode and proton exchange membranes (5), and to control the microbial ecosystem in the anode chamber of the MFC (5-8).

Microbial communities in MFCs are formed corresponding to the electron donors (9-12). Therefore, how do we control the microbial community for efficient production of electricity in practical MFCs supplied with complex organic wastes? It is controversial for effects of external resistances on the performance of MFCs: the external resistance (R_{ext}) affects not only the anode potential (E_{an}) but also the anode biofilm communities, affecting current generation (13-16). For example, Aelterman et al. reported that E_{an} (0, −0.20, and −0.40 V vs. Ag/AgCl) did not affect the start-up time or the final power outputs during a period of approximately 1 month (17). Although anode-respiring bacterial (ARB) communities were grown at different E_{an} (−0.06 to 0.62 V vs. Ag/AgCl), their current outputs were similar under all conditions (18). Further, constant positive potential enables effective acclimatization of ARBs in MFCs, resulting in a faster start-up faster (19). In contrast, a more positive E_{an} (+0.37 V vs. standard hydrogen electrode [SHE]) generates highly diverse communities on the anode, with a low proportion of *Geobacter sulfurreducens*, and produces low current density, whereas

72 more negative E_{an} (−0.15 and −0.09 V vs. SHE) preferentially selects *G. sulfurreducens*
73 and results in high current density (15). Thus, it appears that a more negative E_{an}
74 generates a high proportion of *Geobacter* and low-diversity communities on the anode,
75 resulting in effective production of electricity from MFCs.

76 Since in the practical application MFCs are connected to devices for supplying
77 electricity, it is important to understand the effects of external resistance on the
78 performance of MFCs. The external resistance constrains the flux of electrons, which
79 has significant impacts on the both of performance of MFCs and on its bacterial
80 communities. The objective of this study was to evaluate the effects of external
81 resistance on the electrochemical performance of MFCs and on their microbial
82 community structures. We constructed two MFCs, namely a low resistance-MFC
83 (LR-MFC) and a high-resistance MFC (HR-MFC), with external resistance of 10 Ω and
84 1000 Ω, respectively. We discuss why the performance of the HR-MFC was better than
85 that of the LR-MFC from the perspective of microbial adaptation.
86
87 ## MATERIALS AND METHODS
88
89 **MFC configuration and operation.** A mediator-less air-cathode MFC (8) (Fig.
90 S1) was used to evaluate power generation by microbial communities derived from the
91 sediment of Lake Sanaru (Hamamatsu City, Shizuoka Prefecture, Japan). A carbon
92 paper electroplated with platinum (0.5 mg cm^{-2}) on one side was used as the cathode
93 electrode (CHEMIX Co., Ltd., Sagamihara, Japan), thereby providing a total projected
94 cathode surface area (on one side) of 4 cm^2. A proton exchange membrane (Nafion 117,
95 DuPont, Delaware, USA) was placed between the anode and the cathode. Graphite felt
96 strips (SOHGOH-C Co., Ltd. Yokohama, Japan) were used as the anode (4 cm × 4 cm ×

97 0.5 cm) and were packed in the anode chamber (36 mL capacity) to provide a projected
98 anode surface area of 40 cm^2 without a headspace.
99 The lake sediment (0.4 g) was inoculated into a MFC containing BE medium (5),
100 which is a modification of DHE2 medium (20) and the medium reported by Ishii et al.
101 (21). The BE medium contained 0.5 g KH_2PO_4, 0.2 g $MgSO_4 \cdot 7H_2O$, 0.15 g
102 $CaCl_2 \cdot 2H_2O$, 0.5 g NH_4Cl, 2.5 g $NaHCO_3$, 20 mM sodium lactate, 1.0 mL trace element
103 SL8 solution (22), 1.0 mL Se/W solution (23), and 1.0 mL vitamin solution PV1 (24) per
104 liter. Lactate (electron donor) was added to 20 mM in the anode whenever the cell
105 voltage decreased to baseline. The MFC was incubated under batch conditions with
106 stirring. To compare the effect of external resistance on the generation of electricity,
107 two types of MFCs were constructed, with a different external resistances 10 Ω (called
108 the LR-MFC) and 1000 Ω (the HR-MFC), respectively. Construction of the MFCs was
109 otherwise the same.
110 **Electrochemical analyses.** MFC voltage (V) was recorded every 5 min across a
111 resistance (R) using a data logger (GL200A, Graphtec, Tokyo, Japan) connected to a
112 computer. To evaluate MFCs performance, a polarization curve was determined using a
113 potentiostat (HAV-110, Hokuto Denko Co. Ltd., Japan) set to 2 mV min^{-1} of a slope
114 range within an appropriate interval. MFC performance indices (open-circuit voltage
115 [V_{OC}], short-circuit current density per projection surface area (40 cm^2) of the anode
116 electrode [I_{max}], maximum power density per the projection surface area of the anode
117 electrode [P_{max}], and internal resistance [R_{int}]) were calculated from the slopes of the
118 polarization curves.
119 In chronopotentiometry (CP) and low-scan cyclic voltammetry (LSCV) analyses, an
120 Ag/AgCl reference electrode (HX-R6; 0.199 V corrected to an SHE; Hokuto Denko Co.
121 Ltd.) was placed into the anode chamber to determine the electrode potential. When the

122 E_{an} was measured by CP analysis using a potentiostat (HAV-110, Hokuto Denko Co. Ltd.,
123 Japan), the anode and cathode were used as the working and the counter electrodes,
124 respectively. CP analysis was performed at appropriate intervals of current using the
125 potentiostat. Simultaneously, CP analysis is able to evaluate the performance of
126 electrodes known as limiting current density, which is able to distinguish which
127 electrodes is the limiting factor for producing electricity in a MFC (21). When the
128 cathode was evaluated by CP analysis, the cathode and anode were used as the working
129 and the counter electrodes, respectively. When LSCV analysis was conducted, the
130 anode and cathode were used as the working and counter electrodes, respectively.
131 LSCV was performed at a scan rate of 1 mV s^{-1} between −500 mV and 700 mV vs. SHE.
132 Onset potential was defined as the most negative potential in a Tafel plot (Fig. S2),
133 indicating the most negative potential in stable extracellular electron transfer from
134 microbial cells to the anode. When a sigmoidal curve such as the Nernst-Monod model
135 (7, 25) was observed in the LSCV, a half-saturation potential (E_{KA}), which is the potential
136 at half-maximum current density (13), was estimated from the LSCV curve. The
137 Ag/AgCl reference electrode was placed in the MFC 30 min before performing the CV
138 and CP analyses to allow the electrode to stabilize.

139 **Bacterial community analyses.** The anolytic culture (1.0 mL or 2.0 mL) was
140 directly sampled from the anode compartment of the MFC and bacterial cells were
141 collected by centrifugation for 5 min at 4°C and 20,000 ×*g*. Sections of anode (5 mm ×
142 5 mm × 5 mm) were cut off for bacterial community analyses of biofilm on the anode.
143 The total projection surface area of the cut off portion of the anode was 1.5 cm^2. These
144 sections were washed gently with sterilized sodium-phosphate buffer solution (10 mM,
145 pH 7.0) and were stored at −20°C until DNA extraction, which was used. DNA was
146 extracted according to the conventional method (20).

147 Bacterial community structures were analyzed using a library of cloned 16S rRNA
148 genes. The sediment of Lake Sanaru was used as the inoculum and analyzed on day 0.
149 Anolytic cultures (1 mL or 2 mL) and anodes were collected from MFCs on days 197,
150 333, 427, and 564. Two sections (5 mm × 5mm × 5mm) were cut off from the anode in
151 a glove box in anaerobic conditions. After taking the sections of the anode, new
152 sections of the graphite felts were attached to original anode with a platinum wire.
153 Fragments of 16S rRNA genes were amplified using the primers
154 5′-AGAGTTTGATCCTGGCTCAG-3′ (corresponding to the *Escherichia coli* 16S rRNA
155 gene nucleotide positions 8–27 [26] and 5′-AAGGAGGTGATCCAGCC-3′
156 (corresponding to *E. coli* 16S rRNA gene nucleotide positions 1525–1542).
157 Amplification was performed using a thermal cycler PC320 (ASTEC, Osaka, Japan) in a
158 50 μL mixture containing 0.5 U of KOD FX DNA polymerase (TOYOBO Co., Ltd,
159 Osaka, Japan), buffer solution included with the PCR kit, 400 μM each deoxynucleoside
160 triphosphate, 15 pmol each primer, and 50 ng template DNA. The PCR conditions were
161 2 min for activation of the polymerase at 94°C and then 25 cycles of 1 min at 94°C, 1
162 min at 53°C, and 1 min at 72°C, and finally 10 min extension at 72°C. The PCR
163 products were checked using electrophoresis through 1.5% (w/v) agarose gels in TAE
164 buffer (27); gels were stained with GelRed (Wako, Japan). PCR products were cloned
165 into the vector pTA2 and introduced into competent *E. coli* DH5α cells using a TArget
166 Clone-Plus kit (TOYOBO Co. Ltd., Osaka, Japan) according to the manufacturer's
167 recommendations. Clones were isolated by screening for blue or white phenotypes of
168 bacteria that were incubated in TB medium supplemented with kanamycin (50 mg L^{-1}).
169 Plasmid DNA was extracted using a Wizard Minipreps DNA Purification System
170 (Promega, Madison, WI, USA) according to the manufacturer's directions. The DNA
171 was digested with *Eco*RI and electrophoresed to confirm the expected sizes of the

amplicons. In total, 956 clones were analyzed.

Bacterial community structures were analyzed using denaturing gradient gel electrophoresis (DGGE) analysis targeting 16S rRNA genes. The variable region V3 of the bacterial 16S rRNA gene (corresponding to nucleotide positions 341–534 in the *E. coli* sequence) was amplified using primers P2 and P3 (containing a 40-bp GC clamp [28]) and a thermal cycler PC320 as described previously (20). A Dcode DGGE system (Bio-Rad Laboratories, Inc. CA., USA) was used as recommended by the manufacturer. The PCR-amplified mixture (10 μL) was subjected to electrophoresis through a 10% (w/vol) polyacrylamide gel at 200 V for 3.5 h at 60°C. Gel gradients used for separation, which were applied in parallel to the direction of migration, were 35%–55%. After electrophoresis, the gel was stained with SYBR Green I (FMC Bioproducts) for 30 min as recommended by the manufacture.

The intensity of bands in the DGGE gel was measured using a Gel Doc XR+ system (Bio-Rad), and band intensities were subjected to multidimensional scaling (MDS) analysis. DGGE analysis is not necessarily reproducible. Therefore, the intensities and locations of the DGGE bands were compensated by comparing them with the intensities and locations of common samples electrophoresed through different DGGE gels (Fig. S3). MDS analysis based on the Bray–Curtis index was used to analyze the dynamics of the bacterial community structure, because this index is recognized as one of the most useful methods for evaluating the differences among populations (29, 30). The equation used to calculate the Bray-Curtis index was as follows:

$$\delta_{AB} = (\sum | n_A - n_B |) / [\sum (N_A + N_B)\,] \quad 0 \le \delta_{AB} \le 1,$$

where δ_{AB} represents the dissimilarity index between communities A and B, n_A and n_B represents the intensities of DGGE bands in clusters of A and B, respectively, and N_A and N_B represent the total intensities of DGGE bands in A and B, respectively (30-32). For

197 example, “the dissimilarity index of the anolytic community in the LR-MFC” means the
198 average of dissimilarity indices among all communities in the anolytic community in the
199 LR-MFC. MDS analysis and cluster analysis were conducted using the R v2.12.1 (The
200 R Project for Statistical Computing: http://www.r-project.org/; University of Tsukuba,
201 Japan: http://cran.md.tsukuba.ac.jp) (33). Commands used in R v2.12.1 are shown in
202 Figure S4. The 3D graph was generated using the RINEARN Graph 3D v.5.2.0
203 software.

204 **Nucleotide sequence and phylogenetic analyses**. Cloned genes were sequenced
205 using an ABI PRISM BigDye Terminator version 3.1 Cycle Sequencing Kit and analyzed
206 using an ABI PRISM 3100-*Avant* genetic analyzer (Applied Biosystems, CA, USA).
207 Sequence data were compiled using the GENETYX-MAC program (GENETYX
208 Corporation, Tokyo, Japan). 16S rRNA gene sequence data of chimeras was analyzed
209 using the CHIMERA_CHECK version 2.7 and compared with those retrieved from the
210 Ribosomal Database Project II (34). Sequence data were compared using the BLAST
211 homology search system with those deposited in databases. Multiple sequence
212 alignments and calculations of the nucleotide substitution rate using Kimura’s
213 two-parameter model (35) were performed using the CLUSTAL W program (36).
214 Distance-matrix trees were constructed using the neighbor-joining method (37), and the
215 topologies of the trees were evaluated by bootstrapping with 1,000 resamples (38).

216 **Real-time PCR analysis of *Geobacter* spp.** A real-time PCR assay was applied to
217 genomic DNA to measure 16S rRNA gene copy numbers of *Geobacteraceae* in biofilm
218 on the anode. The DNA extracted for bacterial community analyses was used as
219 template DNAs in this experiment. Standard DNA fragments were produced using a
220 cloned DNA affiliated with the *G. metallireducens* clade. All *Geobacteraceae* clones
221 detected in this study were classified into the *G. metallireducens* clade (Fig. S5).

222 Therefore new specific primers were designed according to the alignment of the
223 *Geobacter* 16S rRNA gene sequences obtained from these experiments with those
224 deposited in GenBank; New *Geo*-f (5′-CGTACCATTAGCTAGTTGGTG-3′) and New
225 *Geo*-r (5′- GATCAAGAGGTATTAGCTCC-3′). Since this set of primers could
226 amplify 16S rRNA genes from cloned DNA affiliated with the *G. metallireducens* clade
227 but could not amplify the 16S rRNA genes of *G. sulfurreducens* PCA which is closest
228 related strain to the *G. metallireducens* clade, the specificity of the set of primers was
229 confirmed (Fig. S6). Real-time quantitative PCR was performed as follows: 95°C for
230 10 min, then 40 cycles of denaturation at 95°C for 10 s, annealing at 65°C for 5 s and
231 extension at 72°C for 15 s. Fluorescence was detected at 86°C for 1 s during each cycle,
232 and a melting curve was generated by heating the product to 95°C and cooling to 40°C.
233 The reaction was performed using a LightCycler FastStart DNA Master SYBR GREEN I
234 kit (Roche Molecular Biochemicals, Indianapolis, IN, USA) and a LightCycler System
235 (Roche Diagnostics, Mannheim, Germany) according to the manufacturer's instructions.
236 The copy numbers of amplicons were calculated using LightCycler software version
237 3.52.

238 **Chemical analysis.** Liquid samples including small particles were collected from
239 the effluent solution of the MFCs. These liquid samples were also filtered (Millipore
240 LG [pore size; 0.2 μm, diameter; 13 mm], Millipore Corporation, Billerica, MA, USA)
241 for quantification of organic acids using an HPLC equipped with a Shodex RSpak
242 KC-811 column (300 × 8.0 mm) (SHOWA DENKO Co. Ltd., Kanagawa, Japan) and a
243 UV detector. The column heater was set to 50°C, samples were eluted using 0.1%
244 H_3PO_4 solution delivered at 1.0 mL min^{-1}, and elutes were monitored at 210 nm.
245 Formate, pyruvate, lactate, butyrate and acetate were identified according to their
246 retention times, and concentrations were determined by comparing the peak area with

247 that of the cognate standard sample.

248 **Accession numbers.** The nucleotide sequences reported here have been deposited
249 in the DDBJ under accession numbers LC000741–LC001696.

250

251 ## RESULTS

252

253 **Electricity generation.** The power densities of both MFCs were monitored (Fig. 1).
254 The power density of the LR-MFC was 4.8 ± 2.5 mW m^{-2} until approximately day 150,
255 after which the maximum power density reached approximately 620 mW m^{-2} from day
256 152 to day 187. The power density decreased and stabilized at 5.2 ± 1.6 mW m^{-2} after
257 day 197. In contrast, the power density of the HR-MFC increased and stabilized at 28 ±
258 9.6 mW m^{-2} after day 197. Coulombic efficiencies of the LR-MFC and the HR-MFC
259 were 21 ± 15% and 18 ± 8%, respectively, after day 197. Acetate and propionate were
260 the main organic acids detected in the LR-MFC, whereas acetate was the main organic
261 acid in the HR-MFC (Fig. S7).

262 **Electrochemical properties.** The electrochemical properties of both MFCs were
263 characterized using three electrochemical analytical methods. Polarization curve
264 analyses showed that the electrochemical properties of both MFCs were similar until day
265 87 (Table S1). However, the electrochemical properties of P_{max} and R_{int} differed after
266 day 197. P_{max} and R_{int} of the LR-MFC were 24 ± 15 mW m^{-2} and 1070 ± 1420 Ω,
267 respectively, whereas those of the HR-MFC were 56 ± 30 mW m^{-2} and 220 ± 145 Ω,
268 respectively. P_{max} and R_{int} of the HR-MFC were approximately 2.3-fold and 0.2-fold
269 those for the LR-MFC, indicating that a higher R_{ext} facilitated improved MFC
270 performance.

271 CP analyses showed that the limiting current densities of the anodes were always

lower than those of the cathodes of both MFCs, indicating that the limiting factor was the anode reactions in the MFCs (Fig. S8). The limiting current density of the anode in both MFCs tended to increase with incubation time. The maximum limiting current densities of the anodes were approximately 1040 mA m^{-2} in the LR-MFC (on day 400) and 1500 mA m^{-2} in the HR-MFC (on day 568). The E_{an} of the LR-MFC ranged from −80 mV to −200 mV at 300 ± 200 mA m^{-2} after day 197, whereas that of the HR-MFC ranged from −220 mV to −280 mV at 90 ± 30 mA m^{-2} after day 197 (Fig. S8).

Most LSCV data (Fig. S9) were not consistent with the Nernst–Monod curve with the exception of the CV data on day 399 (Fig. S9F and S9N). The E_{KA} values of the LR- and HR-MFC on day 399 were estimated to be −116 mV and −200 mV, respectively. $E^{0'}_{an}$ values of the LR-MFC and HR-MFCs were −244 ± 34.2 mV and −254 ± 9.16 mV, respectively (Table 1). The onset potentials of the LR-MFC and the HR-MFC were −206 ± 29.3 mV and −235 ± 21.6 mV, respectively (Table 1).

Phylogenetic analysis and population dynamics of *Geobacter*. *Geobacter* spp. are high current-producing bacteria, and it was therefore important to analyze the population dynamics of *Geobacter* spp. Phylogenetic analysis was performed with 76 clones related to *Geobacter* spp. from the lake sediment as inoculum and anolytic and biofilm samples of the LR- and HR-MFCs (Fig. S5). The analyzed clones were not related to *Geobacter* subsurface clades I, II, or to a novel *Geobacter* clade (8, 39), but belonged to the *G. metallireducens* clade. These clones were grouped into two clusters, including mosaic clones obtained from both MFCs. Based on the phylogenetic analysis, a new set primers was designed to enumerate *Geobacteraceae* in both MFCs, because specific sets of primers reported previously did not detect the *Geobacteraceae* populations of both MFCs.

Real-time PCR analyses revealed that the population dynamics of *Geobacteraceae*

297 differed between the MFCs (Fig. 2). Although *Geobacteraceae* were not detected in
298 either MFC on days 28 and 140, the population density of *Geobacteraceae* then increased
299 and remained constant at $4.7 \pm 2.5 \times 10^6$ copies cm^{-2} from days 258 to 429 in the
300 LR-MFC and $2.8 \pm 0.63 \times 10^6$ copies cm^{-2} from days 197 to 366 in the HR-MFC. The
301 *Geobacteraceae* population density in the LR-MFC reached $1.6 \pm 0.13 \times 10^7$ copies cm^{-2}
302 by day 568. In contrast, the *Geobacteraceae* population density in the HR-MFC
303 decreased to $1.3 \pm 0.04 \times 10^5$ copies cm^{-2} by day 429, and increased again to $1.1 \pm 0.03 \times$
304 10^7 copies cm^{-2} by at day 568.

305 **Bacterial community structure.** Clonal analyses targeting the 16S rRNA genes
306 were performed to investigate the bacterial community structure in the sediment of Lake
307 Sanaru, which was used as the inoculum, as well as those of the anolytic and biofilm
308 communities in the LR-MFC and the HR-MFCs (Fig. 3). The sequence analyses are
309 summarized in Supplemental material Table S2. The community structure of the
310 sediment from Lake Sanaru was more diverse than those of other samples. The
311 proportions of α-, β-, γ-, and δ-*proteobacteria* among the analyzed clones obtained from
312 the anolytic communities were approximately both 73 ± 18% in both MFCs, whereas
313 those in the biofilm communities were 57 ± 19% in the LR-MFC and 51 ± 19% in the
314 HR-MFC.

315 The α-*proteobacteria* represented one of the major dominants of the phylum
316 *Proteobacteria* in the LR-MFC, except for sample of L427B (where L indicates the
317 LR-MFC and B indicates the biofilm). Although a clone closely related to
318 *Rhodopseudomonas palustris* was not detected in the anolytic community in the LR-MFC
319 on day 197 (L197A), such clones represented over 60% of the α-*proteobacteria*
320 community in the anolytic communities of the LR-MFC after day 197. In contrast, the
321 clone represented over 50% of the biofilm population on days 197 (L197B) and day 333

322 (L333B), but less than 30% on days 427 (L427B) and day 564 (L564B). These data
323 indicated that the dynamics of a bacterium closely related to *R. palustris* were different in
324 the anode solution and the biofilm of the LR-MFC.

325 The β-*proteobacteria* represented one of major dominants of the *Proteobacteria* in the
326 HR-MFC, except in samples H427A (where H indicates the HR-MFC and A indicates the
327 anolytic solution) and H197B. Two clones closely related to *Thauera linaloolentis* and
328 *Azoarcus* sp. GPTSA12 represented over 55% of the β-*proteobacteria* in the HR-MFC,
329 except in samples H197A and H427A. The population dynamics of *Thauera* and
330 *Azoarcus* were similar to each other in the HR-MFC.

331 The proportion of δ-*proteobacteria* in biofilm communities was higher compared with
332 those in the anolyte communites of both MFCs. The δ-*proteobacteria* comprise
333 *Geobacter*, *Desulfovibrio*, and *Desulfomicrobium*. The number of clones and
334 proportion of *Geobacter* to δ-*proteobacteria* in the biofilm of the LR-MFC was higher
335 compared with those of the HR-MFC. The proportion of *Firmicutes* of the analyzed
336 clones of anolytic communities in the LR-MFC and HR-MFC were 20 ± 13% and 17 ±
337 16%, respectively, whereas their proportions of the biofilm communities in the LR-MFC
338 and HR-MFC were 36 ± 19% and 38 ± 16%, respectively. Although *Firmicutes* is a
339 very diverse group, these clones were closely related to *Anaerovibrio burkinabensis*
340 DSM6283^{T}, *Acetobacterium submarinus*, and *Acetobacterium*. sp. HAAP-1, which
341 represented 50%–94% of the *Firmicutes* in both MFCs.

342 **Bacterial community dynamics.** MDS analyses based on DGGE profiles were
343 performed to understand the dynamics of the bacterial communities in the both MFCs
344 (Fig. 4 and Fig. S3). The stress value was 0.165, less than 0.20, which means that these
345 data were valuable statistically. The biofilm communities of both MFCs developed
346 individually after day 17, and the dynamics of the anolytic and biofilm communities were

347 synchronous in both MFCs. MDS analyses revealed that bacterial community of the
348 LR-MFC and HR-MFC changed with two stable conditions.. As shown circular
349 shadows (LR-I, LR-II, HR-I, and HR-II) in figure 4, two stable conditions of bacterial
350 community were observed in the LR- and the HR-MFCs, respectively. The dissimilarity
351 indices of the communities in the LR-MFC and the HR-MFC were 0.68 ± 0.15 and 0.69
352 ± 0.17, respectively. The dissimilarity indices values of the anolytic and biofilm
353 communities in the LR-MFC were 0.70 ± 0.14 and 0.56 ± 0.13, respectively, whereas
354 those in the HR-MFC were 0.69 ± 0.18 and 0.57 ± 0.15, respectively.
355
356 **DISCUSSION**
357
358 Here we investigated the effects of external resistance on the performance of air-cathode
359 MFCs using electrochemical and microbial ecological techniques. It is important for the
360 practical application of MFCs to understand integrally how microbial communities adapt
361 to external resistance, because symbiosis between fermenters and ARB contributes to the
362 sustainable performance of MFCs (8, 40); however, this is not presently well understood.
363 Since it is reported that there is a positive correlation between MFC performance and
364 the population density of *G. metallireducens*, a high electricity-producing bacterium (8,
365 15, 21), we predicted that the population density of *G. metallireducens* in the HR-MFC
366 would be higher than that in the LR-MFC. However, the population density of *G.*
367 *metallireducens* in the HR-MFC was similar to or lower than that in the LR-MFC after
368 day 258, and, in particular, the population density of *G. metallireducens* in the HR-MFC
369 significantly decreased from days 366 to 429 (Fig. 2). Why did the *G. metallireducens*
370 population density decrease during that period, and how did the HR-MFC maintain its
371 power density?

372 The LSCV curves of both MFCs on day 399 were sigmoidal, reflecting a
373 Nernst-Monod relationship (Fig. S9F and S9N), and the E_{KA} values of the LR-MFC and
374 the HR-MFC were approximately −116 mV and −200 mV, respectively. The
375 population of *G. sulfurreducens* becomes significantly limited at more negative potentials
376 (E_{KA} of −150 mV or below) (41, 42), indicating that the population density of *G.*
377 *metallireducens* may have decreased because the bacteria were unable to adapt to the
378 more negative potential. How did the remaining *Geobacter* survive in conditions of
379 more negative potential? Electron transfer from *G. sulfurreducens* to a solid electron
380 acceptor is accomplished by outer membrane cytochrome proteins such as OmcB, OmcE,
381 OmcT and OmcS (43-47), and the formal potential of OmcB is −190 mV vs. SHE (48).
382 Further, the redox properties of *G. sulfurreducence* change in the presence of riboflavin
383 and flavin mononucleotide (49). Diverse microbes secrete flavin-like compounds
384 (50-51), suggesting that the *G. metallireducens* enriched in the MFCs had a flexible
385 respiratory system that could adapt to the negative potentials encountered in the
386 HR-MFC.
387 The power density in the HR-MFC was stable after approximately day 180, although
388 the *G. metallireducens* population density decreased from days 366 to 429. As the
389 explantion, we suggested that another exoelectrogens, well adapted to more negative E_{an}
390 produced the electricity. Clone library analyses showed that an increased population
391 density of *Acetobacterium*, which belongs to the phylum *Firmicutes*, corresponded to the
392 decrease of the population density of *G. metallireducens*. This result is surprising,
393 because previous study suggested that syntrophic interaction between *Geobacter* and
394 *Acetobacterium* improves power production (52). Therefore, we speculate that another
395 exoelectrogen capable of engaging in a syntrophic interaction with *Acetobacterium* and
396 adapted to more negative potentials, would produce the electricity. However, the

identity of this exoelectrogen is unknown and will be the subject of future studies.

It is reported that the diversity of bacterial communities on the anode decreases at more negative potentials (15). However, our clone library analysis suggests that the diversities of bacterial communities were similar in both MFCs (Fig. 3). Since the dissimilarity index of the biofilms was lower than that of the anolytic community in both MFCs, the selective pressure of the external resistance was higher on the bacterial communities of the anode than on those of the anolyte. MDS analyses indicated that the dynamics of the biofilm and anolytic communities changed synchronously in both MFCs, and the dynamics of the bacterial communities in the two MFCs were different from each other (Fig. 4). These results suggest that the adapting processes to external resistance of bacterial communities differed between the LR-MFC and the HR-MFC. So, what is the feature of the external electron transfer (EET) of the exoelectrogen in the HR-MFC? Importantly, the onset potential of the HR-MFC was more negative than that of the LR-MFC (Table 1 and Fig. 5), suggesting that the EET mechanism of the microbial communities differed. The details of the EET mechanisms remains to be investigated.

Interestingly, the increased output of the LR-MFC was observed during days 152−187 (Fig. 1A). However, the extreme increase of the *Geobacter* population density and the specific bacterial community structure did not correspond to the increased current density of the LR-MFC. Since it is reported that the current density of an MFC is improved by adding the conductive materials (53), we hypothesize that microorganism(s) produced conductive materials around or on the surface of the anode at this time, resulting in the increase of current production.

In conclusion, we show here that higher external resistance enabled more effective power production from a MFC. The result was dependent on the presence of microbes that adapted to the higher external resistance. The dynamics of anode biofilms and

422 anolytic communities changed synchronously, indicating that the EET mechanism
423 affected the entire microbial ecosystem in the anode chamber of the MFCs.
424 Interestingly, the onset potential of the HR-MFC was more negative than that of the
425 LR-MFC, suggesting that a novel EET mechanism must adapt to the higher external
426 resistance. The novel EET mechanisms that mediates not only the adaptation to a
427 higher external resistance in the HR-MFC, but also the increase in current production
428 from days 155 to 185 in the LR-MFC, are currently under investigation in our laboratory.
429

430 ## Acknowledgments

431 This research was funded in-part by grants KAKENHI (B) 26281038 and KAKENHI
432 15K12228, Japan as well as by the ALCA project, Japan Science and Technology
433 Agency and Tokai Industrial Technology Foundation (H260304No1).

References

1. **Datar, R., Huang, J., Maness, P. C., Mohagheghi, A., Czernik, S., and Chornet. E.:** Hydrogen production from the fermentation of corn stover biomass pretreated with a steam explosion process, Int, J. Hydrogen Energy, **32,** 932-939 (2007).
2. **Fan, Y., Zhang, Y., Zhang, S., Hou, H., and Ren. B.:** Efficient conversion of wheat straw waste into biohydrogen gas by cow dung compost, Bioresour. Technol., **97,** 500-505 (2006).
3. **Logan, B. E. and Regan, J. M.:** Microbial fuel cells--challenges and applications, Environ. Sci. Technol., **40,** 5172-5180 (2006).
4. **Logan, B. E. and Regan, J. M.:** Electricity-producing bacterial communities in microbial fuel cells, Trends Microbiol., **14,** 512-518 (2006).
5. **Rubaba, O., Araki, Y., Yamamoto, S., Suzuki, K., Sakamoto, H., Matsuda, A., and Futamata, H.:** Electricity producing property and bacterial community structure in microbial fuel cell equipped with membrane electrode assembly, J. Biosci. Bioeng., **116,** 106-113 (2013).
6. **Futamata, H, Bretschger, O., Cheung, A., Kan, J., Rubaba, O., Nealson. K. H.:** Adaptation of soil microbes during establishment of microbial fuel cell consortium fed with lactate, J. Biosci. Bioeng., **115,** 58-63 (2013).
7. **Torres, C. I., Marcus, A. K., Lee, H. S., Parameswaran, P., Krajmalnik-Brown, R., and Rittmann. B. E.:** A kinetic perspective on extracellular electron transfer by anode-respiring bacteria, FEMS Microbiol. Rev., **34,** 3-17 (2010).
8. **Yamamoto, S., Suzuki, K., Araki, Y., Mochihara, H., Hosokawa, T., Kubota, H., Chiba, Y., Rubaba, O., Tashiro, Y., and Futamata. H.:** Dynamics of different bacterial communities are capable of generating sustainable electricity from microbial fuel cell with organic waste, Microbes Environ., **29,** 145-153 (2014).

9. **Jung, S. and Regan. J. M.:** Comparison of anode bacterial communities and performance in microbial fuel cells with different electron donors, Appl. Microbial. Biotechnol., **77,** 393-402 (2007).
10. **Kan, J., Hsu, L., Cheung, A. C. M., Pirbazari, M., and Nealson. K. H.:** Current production by bacterial communities in microbial fuel cells enriched from wastewater sludge with different electron donors, Environ. Sci. Technol., **45,** 1139-1146 (2011).
11. **Kiely, P. D., Rader, G., Regan, J. M., and Logan, B.E.:** Long-term cathode performance and the microbial communities that develop in microbial fuel cells fed different fermentation endproducts, Bioresour. Technol., **102,** 361-366 (2012).
12. **Zhang, Y., Min, B., Huang, L., and Angelidaki, I.:** Electricity generation and microbial community response to substrate changes in microbial fuel cell, Bioresour. Technol., **102,** 1166-1173 (2011).
13. **Jung, S. and Regan, J. M.:** Influence of external resistance on electrogensis, methanogenesis, and anode prokaryotic communities in microbial fuel cells, Appl. Environ. Microbiol., **77,** 564-571 (2011).
14. **Rismani-Yazdi, H, Christy, A. D., Carvey, S. M., Yu, Z., Dehority, B. A., and Tuovinen, O. H.:** Effect of external resistance on bacterial diversity and metabolism in cellulose-fed microbial fuel cells, Bioresour. Technol., **102,** 278-283 (2011).
15. **Torres, C. I., Krajmalnik-Brown, R., Parameswaran, P., Marcus, A. K., Wanger, G. Gorby, Y. A., and Rittmann, B. E.:** Selecting anode-respiring bacteria based on anode potential: phylogenetic, electrochemical, and microscopic characterization, Environ. Sci. Technol., **43,** 9519-9524 (2009).
16. **Virdis, B., Rabaey, K., Zhiguo, Y., Rene, A. R., and Keller, J.:** Electron Fluxes in a microbial fuel cell performing carbon and nitrogen removal, Environ. Sci.

484 Technol., **43,** 5144-5149 (2009).
485 17. **Aelterman, P., Freguia, S., Keller, J. Verstraete, W., and Rabaey, K.:** The anode
486 potential regulates bacterial activity in microbial fuel cells, Appl. Microbiol.
487 Biotechnol., **78,** 409-418 (2008).
488 18. **Finkelstein, D. A., Tender, L. M., and Zeikus, J. G.:** Effect of electorde potential
489 on electrode-reducing Microbiota, Environ. Sci. Technol., **40,** 6990-6995 (2006).
490 19. **Wang, X., Feng, Y., Ren, N., Wang, H., Lee, H., Li, N., and Zhao, Q.:**
491 Accelerated start-up of two-chambered microbial fuel cells: effect of anodic positive
492 poised potential, Electrochimi. Acta, **54,** 1109-1114 (2009).
493 20. **Futamata, H., Yoshida, N. Kurogi, T., Kaiya, S., and Hiraishi, A.:** Reductive
494 dechlorination of chloroethenes by *Dehalococcoides*-containing cultures enriched
495 from a polychlorinated-dioxin-contaminated microcosm, ISME J. **1,** 471-479 (2007).
496 21. **Ishii, S., Watanabe, K., Yabuki, S., Logan, B. E., and Sekiguchi, Y.:** Comparison
497 of electrode reduction activities of *Geobacter sulfurreducens* and an enriched
498 consortium in an air-cathode microbial fuel cell, Appl. Environ. Microbiol., **74,**
499 7348-7355 (2008).
500 22. **Biebl, H. and Pfenning, N.:** Growth yield of green sulfur bacteria in mixed cultures
501 with sulfur and sulfate reducing bacteria, Arch. Microbiol.. **117,** 9-16 (1978).
502 23. **Löffler, F. E., Sanford, R. A. and Tiedje, J. M.:** Initial characterization of a
503 reductive dehalogenase from *Desulfitobacterium chlororespirans* Co23, Appl.
504 Environ. Microbial., **62,** 3809-3818 (1996).
505 24. **Hiraishi, A., Yonemitsu, Y., Matsuhita, M., Shin, Y. K., Kuraishi, H., and**
506 **Kawahara, K.:** Characterization of *Porphyrobacter sanguineus* sp. nov., an aerobic
507 bacteriochlorophyII-containing bacterium capable of degrading biphenyl and
508 dibenzofuran, Arch Microbiol., **178,** 45-52 (2002).

509 25. **Marcus, A. K., Torees, C. I., Rittmann, B. E.:** Conduction-based modeling of the
510 biofilm anode of a microbial fuel cell, Biotechnol. Bioeng., **98,** 1171-1182 (2007).
511 26. **Brosius, J., Dull, T. J., Sleeter, D. D., and Noller, N. F.:** Gene organization and
512 primary structure of a ribosomal RNA operon from *Escherichia coli*, J. Mol. Biol.
513 **148,** 107-127 (1981).
514 27. **Sambrook, J., Fritsch, E.F. and Maniatis. T.:** Molecular cloning: A laboratory
515 manual, 2nd ed. Cold Spring Harbor Laboratory Press, New York, USA. (1989).
516 28. **Müyzer, G., de Waal, E.C. and Uitterlinden. A.G.:** Profiling of complex
517 microbial populations by denaturing gradient gel electrophoresis analysis of
518 polymerase chain reaction-amplified genes coding for 16S rRNA, Appl. Environ.
519 Microbiol., **59,** 695-700 (1993).
520 29. **Clarke, K.R.:** Non-parametric multivariate analyses of changes in community
521 structure, Austral Ecol., **18,** 117-143 (1993).
522 30. **Faith, D. P., Minchin, P. R., and Belbin, L.:** Compositional dissimilarity as a
523 robust measure of ecological distance, Plant Ecol., **69,** 57-68 (1987).
524 31. **Bray, J. R. and Curtis, T. J.:** An ordination of the upland forest communities of
525 southern Wisconsin, Ecol Monogr **27,** 325-349 (1957).
526 32. **Michie, G. M.:** Use of the Bray-Curtis similarity measure in cluster analysis of
527 foraminiferal date, Math. Geosci. **14,** 661-667 (1982).
528 33. **Shiro, S, Yamamoto, A., Umehara, Y., Hayashi, M., Yoshida, N., Nishiwaki, A.,**
529 **Yamakawa, T., and Saeki, Y.:** Effect of *Rj* genotype and cultivation temperature
530 on the community stucture of soybean-nodulating bradyrhizobia, Appl. Envrion.
531 Microbiol., **78,** 1243-1250 (2012).
532 34. **Cole, J. R., Chai, B., Marsh, T. L., Farris, R. J., Wang, Q., Kulam, S. A.,**
533 **Chaudra, S., McGarrell, D. M., Schmidt, T. M., Garrity, G. M., and Tiedje, J.**

M.: The Ribosomal Database Project (RDP-II): previewing a new autoaligner that allows regular updates and the new prokaryotic taxonomy, Nucleic Acids Res., **31,** 442-443 (2003).

35. **Kimura, M.:** A simple method for estimating evolutionary rates of base substitutions through comparative studies of nucleotide sequences, J. Mol. Evol., **16,** 111-120 (1980).
36. **Thompson, J. D., Higgins, D. G., and Gibson, T. J.:** CLUSTAL W: improving the sensitivity of progressive multiple sequence alignment weight matrix choice, Nucleic Acid Res., **22,** 4673-4680 (1994).
37. **Saito, N. and Nei. M.:** The neighbor-joining method: a new method for reconstructing phylogenetic trees, Mol. Biol. Evol., **4,** 406-425 (1987).
38. **Felsenstein, J.:** Confidence limits on phylogenies: an approach using the bootstrap, Evolution, **39,** 783-791 (1985).
39. **Holmes, D. E., O'Neil, R. A., Vrionis, H. A., N'guessan, L. A., Ortiz-Bernad, I., Larrahondo, M. J., Adams, L. A., Ward, J. A., Nicoll, J. S., Nevin, K. P., and other 4 authors.:** Subsurface clade of *Geobacteraceae* that predominates in a diversity of Fe(III)-reducing subsurface environments, ISME J., **1,** 663-677 (2007).
40. **Ishii, S., Suzuki, S., Norden-Krichmar, T. M., Nealson, K. H., Sekiguchi, Y., Gorby, Y. A., and Bretschger, O.:** Functionally stable and phylogenetically diverse microbial enrichments from microbial fuel cells during wastewater treatment. PLoS One **7,** e30495..doi.org/10.1371/journal.pone.0030495 (2012).
41. **Srikanth, S., Marsili, E. Flickinger, M.C. and Bond. D.R.:** Electrochemical characterization of *Geobacter sulfurreducens* cells immobilized on graphite paper electrodes, Biotechnol. Bioeng., **99,** 1065-1073 (2008).
42. **Torres, C. I., Marcus, A. K., Parameswaran, P., and Rittmann, B. E.:** Kinetic

559 experiments for evaluating the Nernst-Monod model for anode-respiring bacteria
560 (ARB) in a biofilm anode, Environ. Sci. Technol., **42,** 6593-6597 (2008).
561 43. **Holmes, D. E., Chaudhuri, S. K., Nevin, K. P., Mehte, T., Methé, B. A., Liu, A.,**
562 **Ward, J. E., Woodard, T. L., Webster, J., and Lovley, D. R.:** Microarray and
563 genetic analysis of electron transfer to electrodes in *Geobacter sulfurreducens*,
564 Environ. Microbiol., **8,** 1805-1815 (2006).
565 44. **Leang, C., Adams, L. A., Chin, K. J., Nevin, K. P., Methe, B. A., Webster, J.,**
566 **Sharma, M. L., and Lovley, D. R.:** Adaptation to disruption of the electron transfer
567 pathway for Fe(III) reduction in *Geobacter sulfureeducens*, J. Bacteriol., **187,**
568 5918-5926 (2005).
569 45. **Leang, C., Coppi, M. V., and Lovley, D. R.:** OmcB, a *c*-type polyheme
570 cytochrome, involved in Fe(III) reduction in *Geobacter sulfurreducens*, J. Bacteriol.,
571 **185,** 2096-2103 (2003).
572 46. **Mehta, T., Coppi, M. V., Childers, S. E., and Lovley, D. R.:** Outer membrane
573 *c*-type cytochromes required for Fe(III) and Mn(IV) oxide reduction in *Geobacter*
574 *sulfurreducens*, Appl. Environ. Microbiol., **71,** 8634-8641 (2005).
575 47. **Richter, H., Nevin, K. P., Jia, H., Lowy, D. A., Lovley, D. R., and Tender, L.**
576 **M.:** Cyclic voltammetry of biofilms of wild type and mutant *Geobacter*
577 *sulfurreducens* on fuel cell anodes indicates possible roles of OmcB, OmcZ, type IV
578 pili, and protons in extracellular electron transfer, Energy Environ. Sci. **2,** 506-516
579 (2009).
580 48. **Magnuson, T. S., Isoyama, N., Hodges-Myerson, A. L., Davidson, G., Maroney,**
581 **M. J., Geesey, G. G., and Lovley, D. R.:** Isolation, characterization and gene
582 sequence analysis of a membrane-associated 89KDa Fe(III) reducing cytochrome *c*
583 from *Geobacter sulfurreducens*, Biochem. J., **359,** 147-152 (2001).

584 49. **Okamoto, A., Saito, K., Inoue, K., Nealson, K. H., Hashimoto, K., and**
585 **Nakamura, R.:** Uptake of self-secreted flavins as bound cofactors for extracellular
586 electron transfer in *Geobacter* species, Energy Envion. Sci. **7,** 1357-1361 (2014).
587 50. **Rabaey, K., Boon, N., Hofte, M., and Verstraete, W.:** Microbial phenazine
588 production enhances electron transfer in biofuel cells, Environ. Sci. Technol., **39,**
589 3401-3408 (2005).
590 51. **Rabaey, K., Boon, N., Siciliano, S. D., Verhaege, M., and Verstraete, W.:**
591 Biofuel cells select for microbial consortia that self-mediate electron transfer, Appl.
592 Environ. Microbiol., **70,** 5373-5382 (2004).
593 52. **Sun, D., Call, D. F., Kiely, P. D., Wang, A., and Logan, B. E.:** Syntrophic
594 interactions improve power production in formic acid fed MFCs operated with set
595 anode potentials or fixed resistances, Biotechnol. Bioeng., **109,** 405-414 (2011).
596 53. **Nakamura, R., Kai, F., Okamoto, A., Newton, G. J., and Hashimoto, K.:**
597 Self-constructed electrically conductive bacterial networks, Angew. Chem. Int. Ed.,
598 **48,** 508-511 (2009).

599 **Figure legends**

600

601 Figure 1. Electricity generation from the MFCs used in this study. (A) MFC with 10 Ω
602 external resistance (LR-MFC). The small graph inserted into figure 1A shows the power
603 density at full range. (B) MFC with 1000 Ω external resistance (HR-MFC).

604

605 Figure 2. Enumeration of the *Geobacteraceae* population density in biofilm samples
606 using real-time PCR with specific primers. Gray symbol and line, LR-MFC; Black
607 symbol and line, HR-MFC. The standard deviation is indicated by an error bars behind
608 the symbols.

609

610 Figure 3. Phylogenetic distribution of 16S rRNA gene clones from soil, anolytic, and
611 biofilm samples in the LR-MFC and the HR-MFC. "S" denotes the inoculum soil sample.
612 The number indicates the sampling date. "L" and "H" above the number denote the
613 LR-MFC and the HR-MFC, respectively. "A" and "B" next to the number denote the
614 anolytic and biofilm samples, respectively. The number above each bar indicates the total
615 number of sequenced clones.

616

617 Figure 4. Multidimensional scaling analyses based on DGGE profiles. Light and dark
618 blue denote anolytic and biofilm communities in the LR-MFC, respectively. Light and
619 dark red denote the anolytic and biofilm communities in the HR-MFC, respectively. The
620 number indicates the sampling date, and "B" next to the number denotes the biofilm sample.
621 Circular shadows (LR-I, LR-II, HR-I, and HR-II) indicate bacterial communities that are in
622 dynamic equilibrium.

623

624 Figure 5. Schematic diagram of the properties of current production illustrating the $E^{0'}$
625 anode and the onset potential with different external resistances.

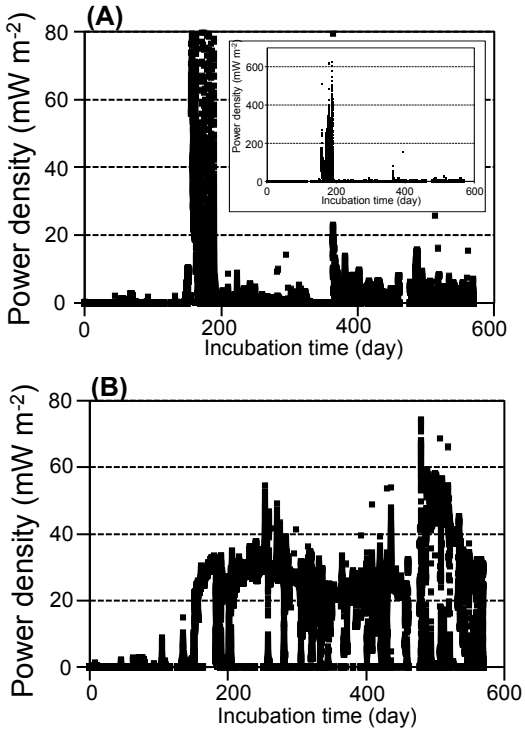

Figure 1 Suzuki et al.

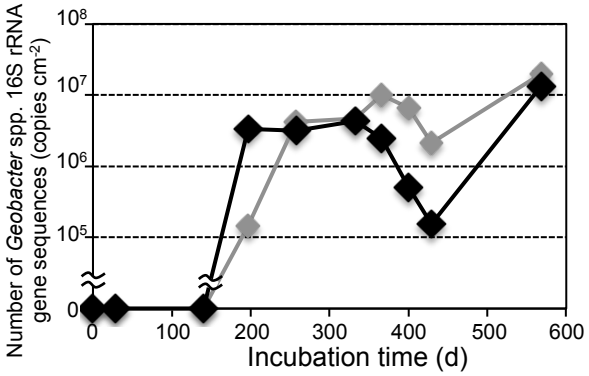

Figure 2 Suzuki et al.

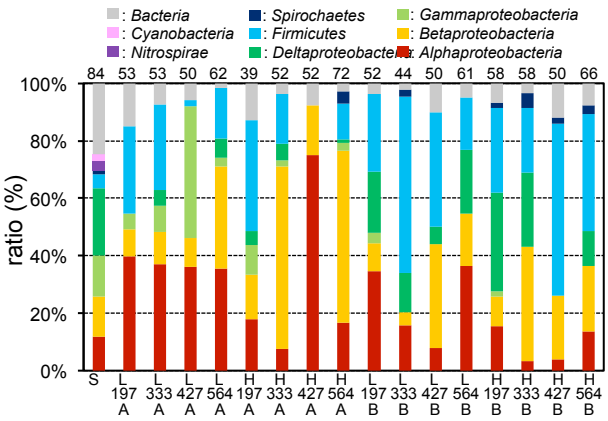

Figure 3 Suzuki et al.

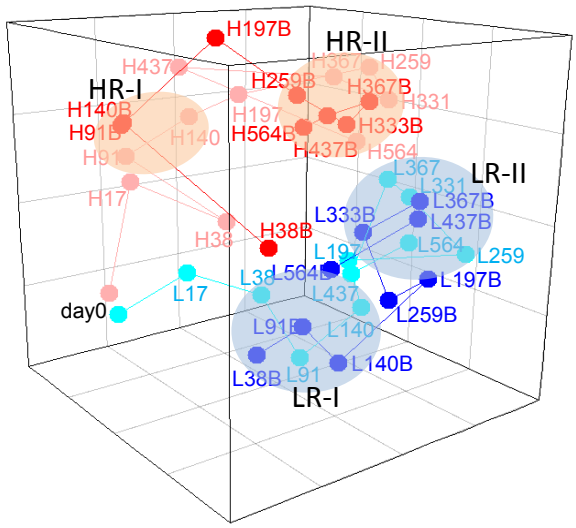

Figure 4 Suzuki et al.

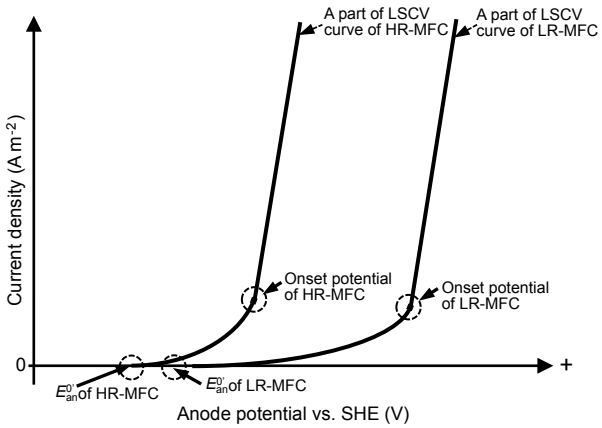

Figure 5. Suzuki et

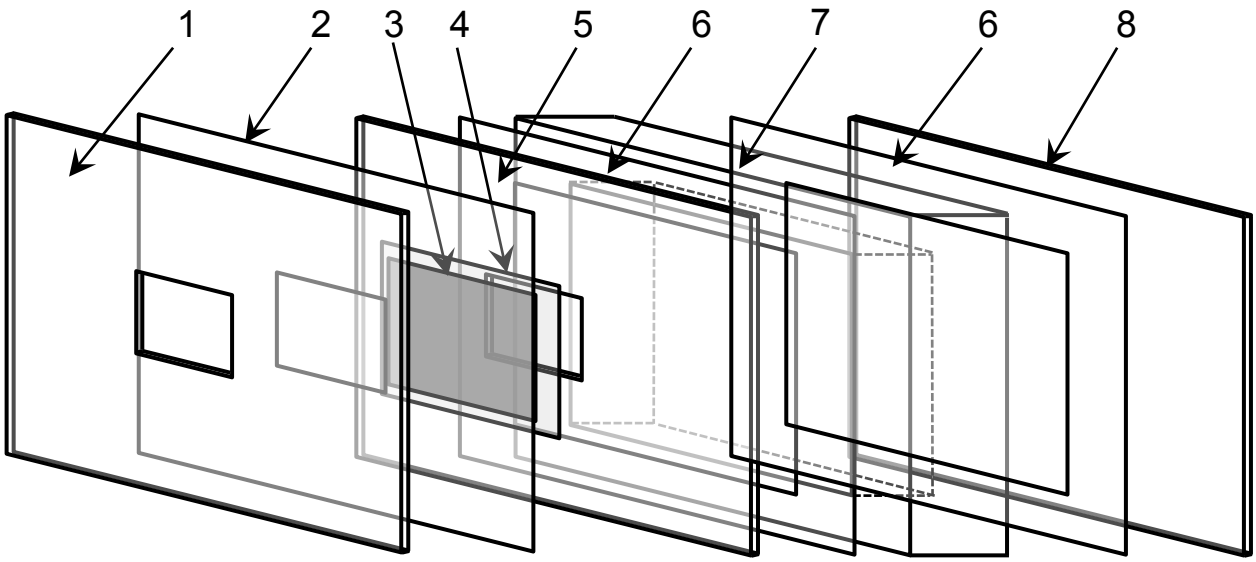

Fig. S1 Suzuki et al.

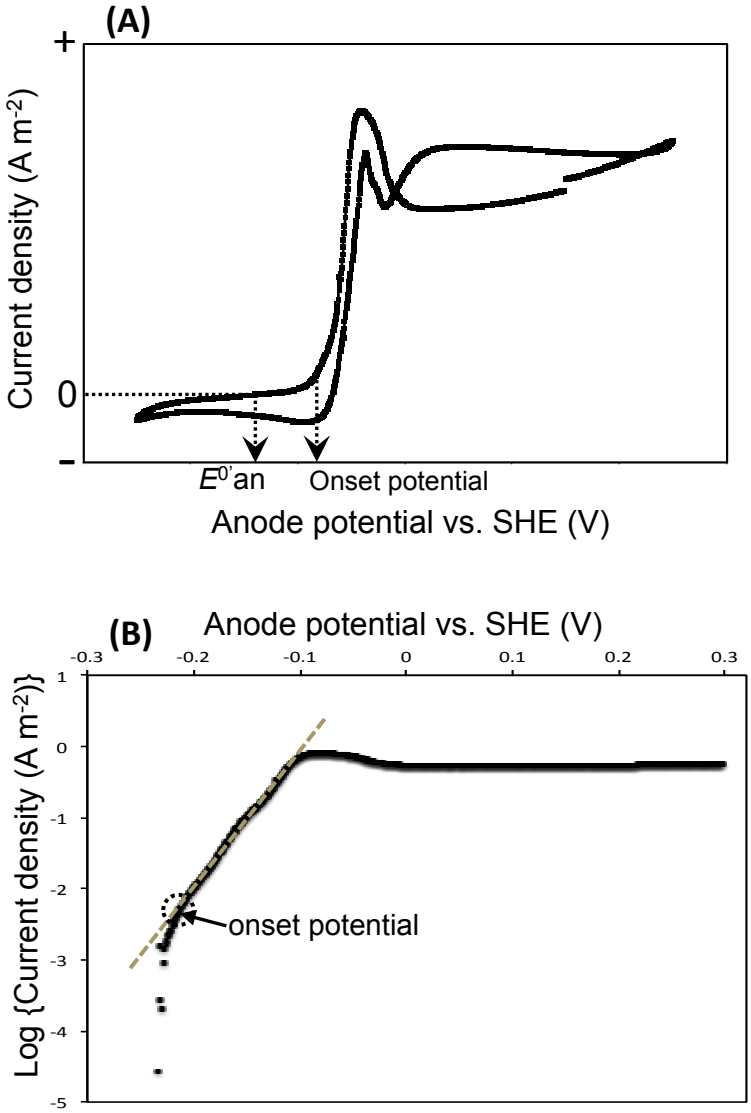

Fig. S2 Suzuki et al.

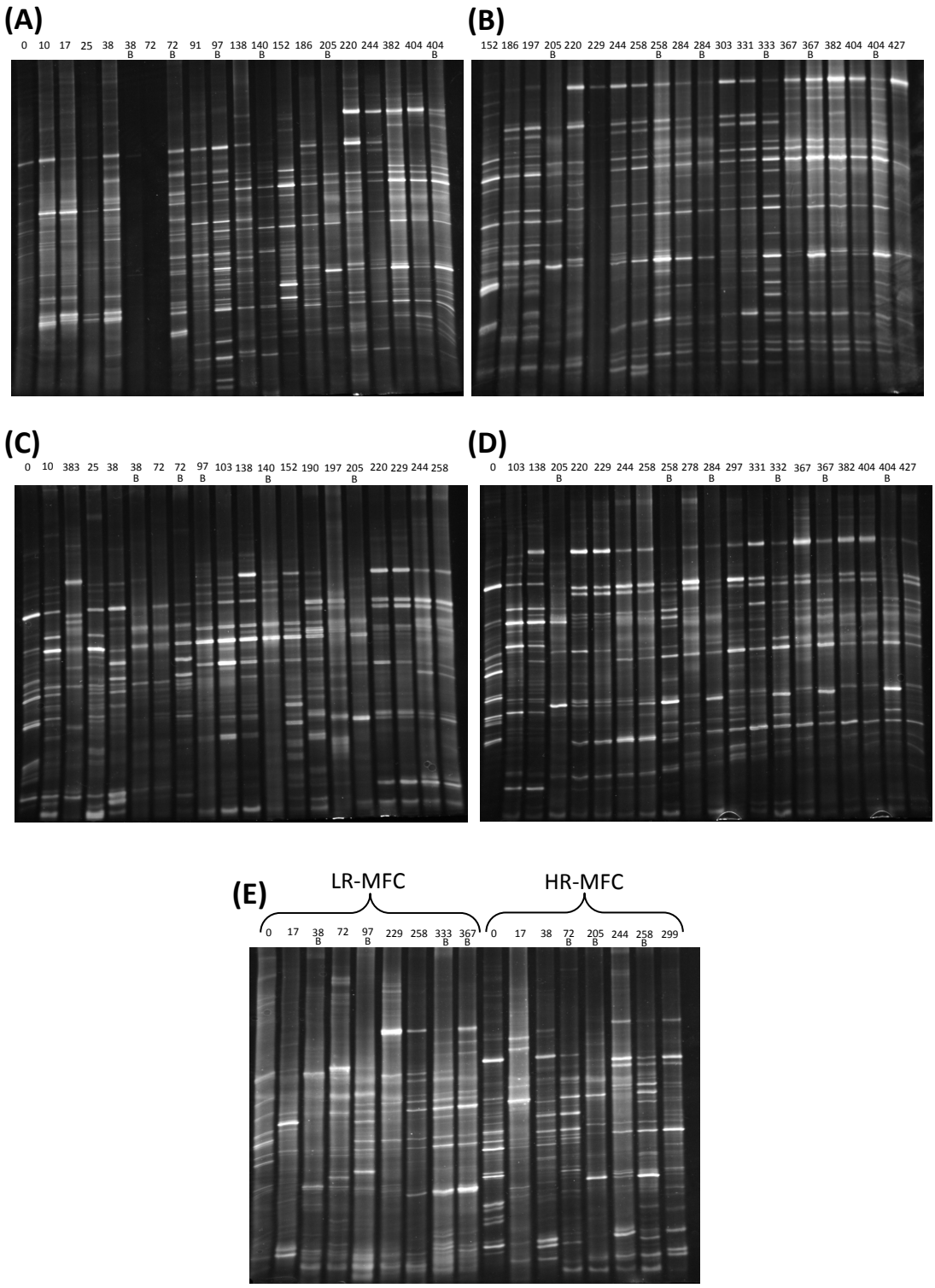

Fig. S3 Suzuki et al.

The program of MDS analysis on R used in this study

```
>library(mvpart)
>read.table("File name.txt")
>x<-read.table("File name.txt")
>gdist(x,method="bray")
>y<-gdist(x,method="bray")
>cmdscale(y,k=3,eig=T)

>library(MASS)
>x<-read.table("File name.txt")
>y<-gdist(x,method="bray")
>mds<-isoMDS(y,k=3)
```

Fig. S4 Suzuki et al.

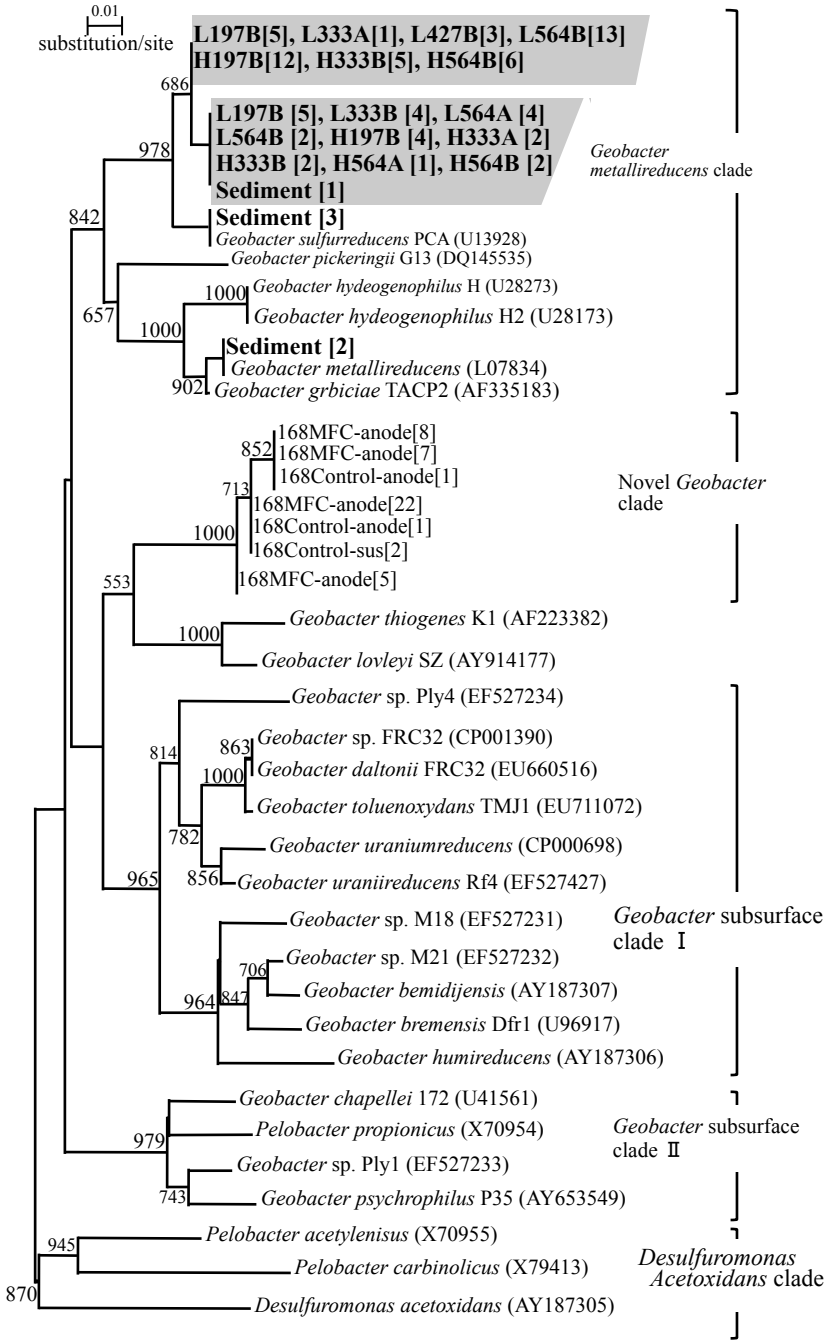

Fig. S5 Suzuki et al.

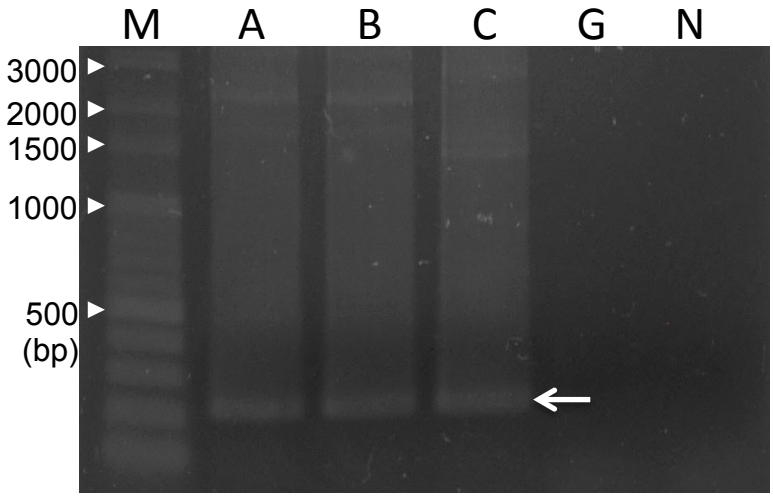

Fig. S6 Suzuki et al.

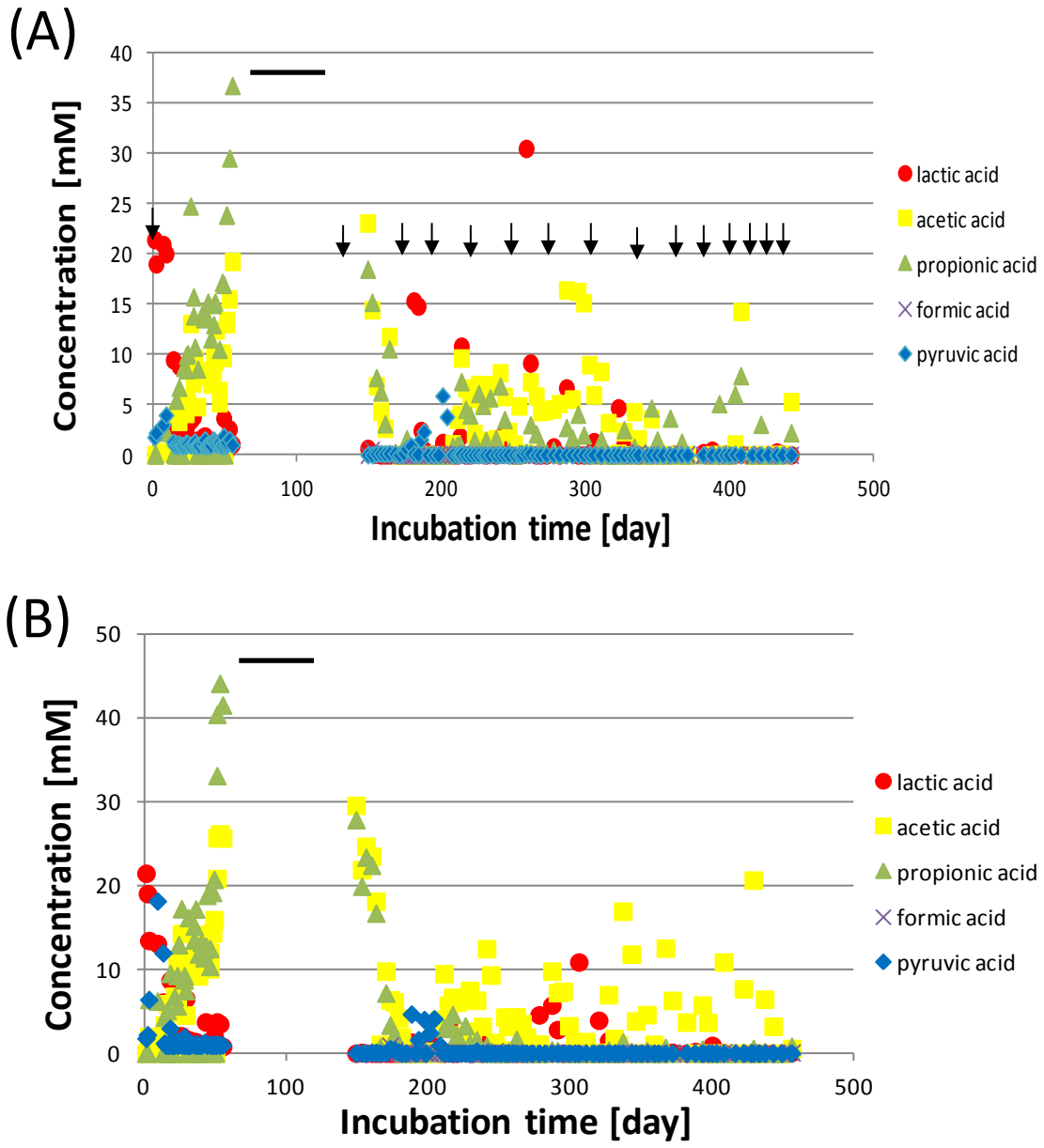

Fig. S7 Suzuki et al.

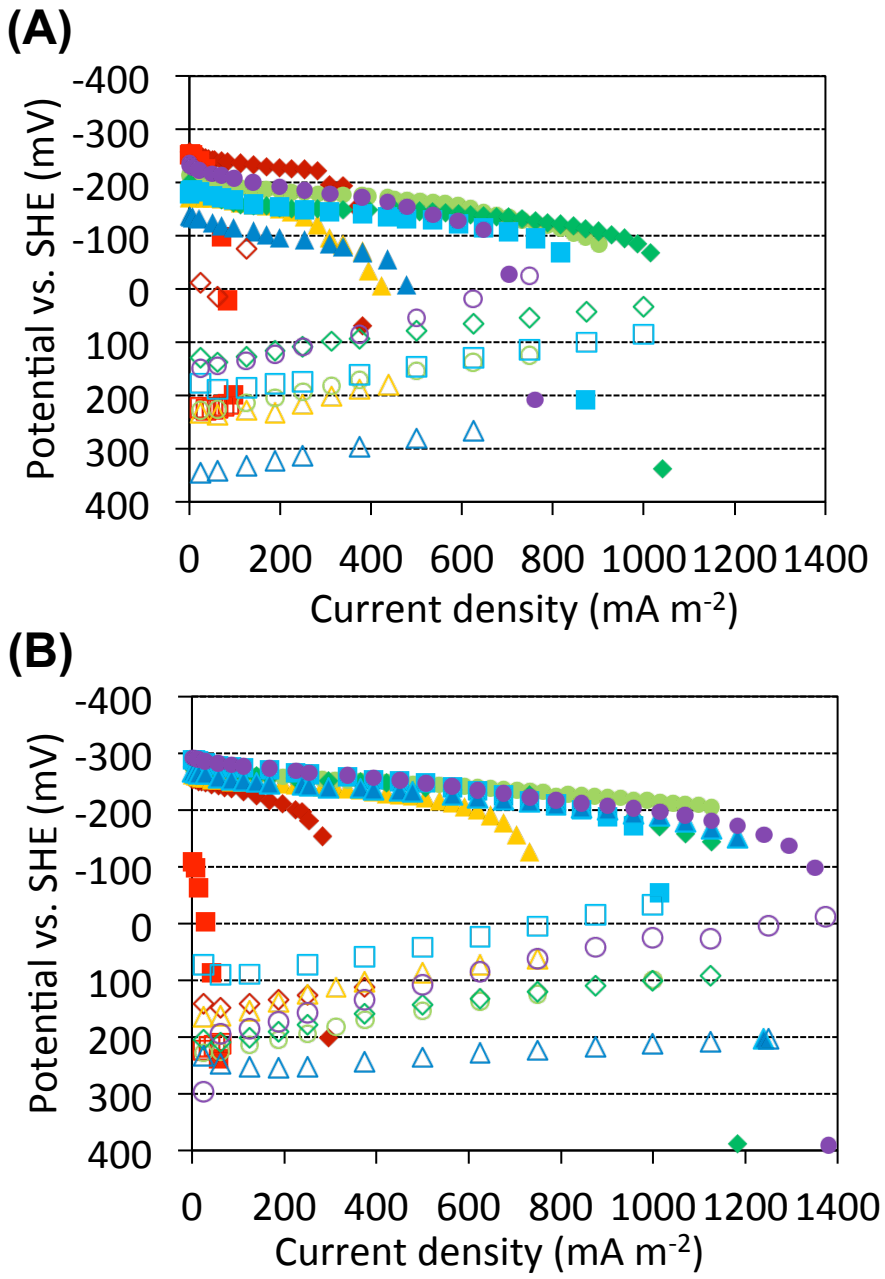

Fig. S8 Suzuki et al.

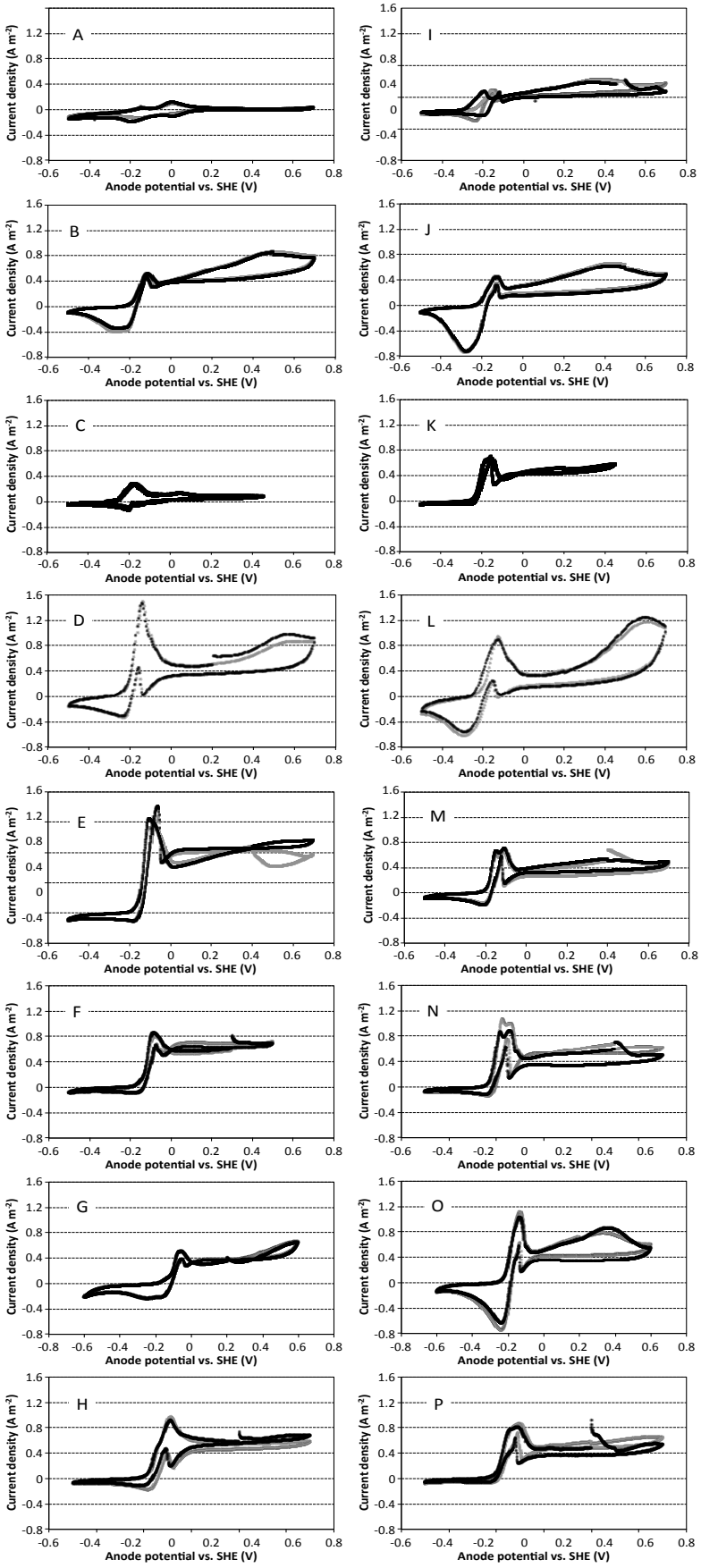

Fig. S9 Suzuki et al.

Table S1. Electrochemical properties of LR- and HR-MFCs by polarization curve analyses

Incubation time (day)	LR-MFC				HR-MFC			
	Voc (mV)	I_{max} (mA m^{-2})	P_{max} (mW m^{-2})	R_{int} (Ω)	Voc (mV)	I_{max} (mA m^{-2})	P_{max} (mW m^{-2})	R_{int} (Ω)
30	280	5.4	0.26	28300	280	5.1	0.26	28300
46	300	6.2	0.47	10300	270	3.8	0.27	23000
87	280	8.3	0.82	11500	200	4.4	0.28	15500
117	230	16	0.90	5000	210	6.3	0.40	12000
157	420	160	1.9	660	320	90	17	470
197	470	35	5.4	3200	430	300	29	430
256	420	90	14	1200	450	750	76	100
332	470	320	23	400	470	450	44	160
366	410	290	35	180	460	560	49	160
400	410	570	44	140	430	740	67	140
429	350	300	19	230	460	600	56	180
478	400	390	28	300	430	260	20	480
493	430	290	40	180	460	570	120	70
576	360	47	3.4	3800	470	700	40	290
Ave±SE[a]	410±42	260±175	24±15	1070±1420	450±17	550±180	56±30	220±145

[a]; Average and SE were caliculated using from day 197 to day 576.

Table S2. List of clones and phylogenetically related organisms

Sediment in Lake Sanaru		
Mostly related microorganism	Number of clone	Phylogenetic phylum
Dehalococcoides sp. BHI80-15	4	*Chloroflexi*
Olavius sp. associated proteobacterium Delta 1	4	*Deltaproteobacteria*
Pseudomonas sp. VT1B	3	*Gammaproteobacteria*
Bacterium WH6-7	2	*Bacteria*
Candidatus Magnetobacterium bavaricum	2	*Nitrospirae*
Comamonas testosteroni partial	2	*Betaproteobacteria*
Dehalogenimonas sp. SBP1	2	*Chloroflexi*
Desulfobacterium anilini strain AK1	2	*Deltaproteobacteria*
Geobacter sulfurreducens KN400	2	*Deltaproteobacteria*
Methylibium sp. UKPF16	2	*Betaproteobacteria*
Thermoanaerobacter sp. ToBE	2	*Firmicutes, Clostridia*
Thiobacillus denitrificans ATCC 25259	2	*Betaproteobacteria*
Thiobacillus denitrificans strain ME16	2	*Betaproteobacteria*
Acidobacteria bacterium IGE-010	1	*Bacteria, Acidobacteria*
Actinobacterium SCGC AAA003-N08	1	*Bacteria, Actinobacteria*
Alpha proteobacterium IMCC1702	1	*Alphaproteobacteria*
Anaerobic bacterium MO-CFX2	1	*Bacteria.*
Anaerobic bacterium sk.prop8	1	*Firmicutes, Clostridia*
Anderseniella baltica partial	1	*Alphaproteobacteria*
Bacterium DY22613	1	*Bacteria*
Bacterium HTCC4091	1	*Bacteria*
Bacterium MP-01	1	*Bacteria*
Bacterium ROME215Asa	1	*Bacteria*
Bacterium WH8-1	1	*Bacteria*
Brevundimonas olei strain IARI-DV-16	1	*Alphaproteobacteria*
Comamonas sp. JC8	1	*Betaproteobacteria*
Coxiella burnetii CbuG_Q212	1	*Gammaproteobacteria*
Cyanobium sp. Suigetsu-CR2	1	*Bacteria, Cyanobacteria*
Cyanobium sp. Suigetsu-CR5	1	*Bacteria, Cyanobacteria*
Defluviimonas sp. BS14	1	*Alphaproteobacteria*
Delta proteobacterium 28bB2T	1	*Deltaproteobacteria*
Delta proteobacterium EtOHpelo	1	*Deltaproteobacteria*
Delta Proteobacterium G50VI partial	1	*Deltaproteobacteria*
Delta proteobacterium SCGC AAA003-K20	1	*Deltaproteobacteria*
Desulfobulbus sp. DSM 2033	1	*Deltaproteobacteria*
Desulfotomaculum acetoxidans DSM 771	1	*Firmicutes, Clostridia*
Desulfovibrio sp. X2	1	*Deltaproteobacteria*
Endosymbiont of Tevnia jerichonana	1	*Gammaproteobacteria*
Gemmatimonadetes bacterium SCGC AAA007-O06	1	*Bacteria*
Gemmatimonas aurantiaca clone H9-0AF4E_11038	1	*Gammaproteobacteria*
Geobacter metallireducens GS-15	1	*Deltaproteobacteria*
Geobacter sp. DSM 9736 partial	1	*Deltaproteobacteria*
Geobacter sp. OSK2A	1	*Deltaproteobacteria*
Geobacter sp. SD-1	1	*Deltaproteobacteria*
Halochromatium sp. MTK6IM088 partial	1	*Gammaproteobacteria*
Hyphomicrobium sp. Ellin112	1	*Alphaproteobacteria*
Leptospira interrogans clone BEL041LA2	1	*Bacteria, Spirochaetes*
Lucina nassula gill symbiont	1	*Gammaproteobacteria*
Modestobacter versicolor strain CP153-2	1	*Bacteria, Actinobacteria*
Olavius algarvensis associated proteobacterium Delta 3 partia	1	*Deltaproteobacteria.*
Pelobacter acetylenicus	1	*Deltaproteobacteria.*
Planctomycetes bacterium SCGC AAA240-E07	1	*Bacteria, Planctomycetes*
Planctomycetes bacterium SCGC AAA240-G14	1	*Bacteria, Planctomycetes*
Pseudorhodobacter ferrugineus	1	*Alphaproteobacteria*
Rhodobacter maris partial	1	*Alphaproteobacteria*
Rhodobacter sp. CR07-5	1	*Alphaproteobacteria*
Rhodobacterales bacterium CB1049	1	*Alphaproteobacteria*
Rhodovulum sp. JC2237	1	*Alphaproteobacteria*
Rubrivivax gelatinosus strain 16	1	*Betaproteobacteria*
Thermanaerothrix daxensis strain GNS-1	1	*Chloroflexi*
Thermodesulfovibrio thiophilus	1	*Nitrospirae*
Thialkalivibrio thiocyanodenitrificans strain ARhD	1	*Gammaproteobacteria*
Thiobacillus thioparus strain THI 111	1	*Betaproteobacteria*
Thiobacillus thioparus strain THI 115	1	*Betaproteobacteria*
Thiococcus pfennigii partial	1	*Gammaproteobacteria*
Xanthomonas sp. P2-12-1 partial	1	*Gammaproteobacteria*
Total clone number	84	

Continued supplemental material Table S2

Anolytic bacterial communities in the LR-MFC at day 197		
Mostly related microorganism	Number of clone	Phylogenetic phylum
Holosporaceae bacterium Serialkilleuse_9403403	7	*Alphaproteobacteria*
Endosymbiont of Acanthamoeba sp. AC305	6	*Bacteria*
Acetobacterium sp. HAAP-1	5	*Firmicutes, Clostridia*
Arsenite-oxidizing bacterium NT-6	2	*Betaproteobacteria*
Brevundimonas sp. LC437	2	*Alphaproteobacteria*
Clostridium sp. SW001	2	*Firmicutes, Clostridia*
Clostridium sp. 6-44	2	*Firmicutes, Clostridia*
Hydrogenophaga sp. AR20 gene	2	*Betaproteobacteria*
Ochrobactrum anthropi strain W-7	2	*Alphaproteobacteria*
Rhodobacter sp. Bo10-19	2	*Alphaproteobacteria*
Thermomonas koreensis strain Ko06	2	*Gammaproteobacteria*
Acetobacterium submarinus	1	*Firmicutes, Clostridia*
Acetobacterium wieringae strain DP9	1	*Firmicutes, Clostridia*
Acidovorax caeni	1	*Betaproteobacteria*
Alpha proteobacterium PI_GH2.1.D7	1	*Alphaproteobacteria*
Anaerovibrio burkinabensis DSM 6283(T)	1	*Firmicutes; Negativicutes*
Azospirillum brasilense	1	*Alphaproteobacteria*
Bosea sp. 1011	1	*Alphaproteobacteria*
Clostridiales bacterium JN18_A89_K*	1	*Firmicutes, Clostridia*
Christensenella minuta	1	*Firmicutes, Clostridia*
Clostridium sticklandii str. DSM 519 chromosome	1	*Firmicutes, Clostridia*
Clostridium sp. PPf35E6	1	*Firmicutes, Clostridia*
Devosia sp. L15	1	*Alphaproteobacteria*
Ochrobactrum anthropi strain X-12	1	*Alphaproteobacteria*
Ochrobactrum sp. DX2	1	*Alphaproteobacteria*
Phenylobacterium falsum	1	*Alphaproteobacteria*
Propionibacterium freudenreichii strain ISU P59	1	*Bacteria, Actinobacteria*
Pseudomonas sp. SgZ-6	1	*Gammaproteobacteria*
Roseomonas sp. R049	1	*Alphaproteobacteria*
Rumen bacterium R-7 gene	1	*Bacteria*
Total clone number	53	

Anolytic bacterial communities in the LR-MFC at day 333		
Mostly related microorganism	Number of clone	Phylogenetic phylum
Rhodopseudomonas palustris	12	*Alphaproteobacteria*
Acetobacterium submarinus	5	*Firmicutes, Clostridia*
Thauera linaloolentis	5	*Betaproteobacteria*
Anaerovibrio burkinabensis DSM 6283(T)	4	*Firmicutes, Negativicutes*
Clostridium sp. 6-44	3	*Firmicutes, Clostridia*
Clostridium sp. SW001	3	*Firmicutes, Clostridia*
Rhodobacter sp. Bo10-19	2	*Alphaproteobacteria*
Rhodobacter sphaeroides strain S10-1	2	*Alphaproteobacteria*
Stenotrophomonas acidaminiphila strain T-15	2	*Gammaproteobacteria*
Azoarcus sp.	1	*Betaproteobacteria*
Azospirillum brasilense partial	1	*Alphaproteobacteria*
Azospirillum sp. TS18	1	*Alphaproteobacteria*
Bacterium ROME195Asa	1	*Bacteria*
Bacterium ROMEm59sa320	1	*Bacteria*
Clostridium sp. AUH-JLC235	1	*Firmicutes, Clostridia*
Desulfovibrio vulgaris str. 'Miyazaki F'	1	*Deltaproteobacteria*
Dietzia natronolimnaea strain LL 51	1	*Bacteria, Actinobacteria*
Geobacter sp. LAR-2	1	*Deltaproteobacteria*
Holosporaceae bacterium Serialkilleuse_9403403	1	*Alphaproteobacteria*
Ochrobactrum sp. DX2	1	*Alphaproteobacteria*
Stenotrophomonas acidaminiphila strain st31	1	*Gammaproteobacteria*
Stenotrophomonas sp. AR34	1	*Gammaproteobacteria*
Unidentified eubacterium from anoxic bulk soil	1	*Bacteria*
Xanthomonas sp. TE9	1	*Gammaproteobacteria*
Total clone number	53	

Continued supplemental material Table S2

Anolytic bacterial communities in the LR-MFC at day 427		
Mostly related microorganism	Number of clone	Phylogenetic phylum
Stenotrophomonas acidaminiphila strain st31	21	*Gammaproteobacteria*
Rhodopseudomonas palustris	13	*Alphaproteobacteria*
Alcaligenes faecalis strain BAB-1832	2	*Betaproteobacteria*
Bacterium KKCSSW	2	*Bacteria*
Comamonas testosteroni partial	2	*Betaproteobacteria*
Rhodobacter sphaeroides strain S10-1	2	*Alphaproteobacteria*
Azorhizobium sp. pcnb-3	1	*Alphaproteobacteria*
Bacterium 14W314	1	*Bacteria*
Bosea sp. CRIB-12	1	*Alphaproteobacteria*
Delftia tsuruhatensis strain M6	1	*Betaproteobacteria*
Lysinibacillus fusiformis strain DZQ17-H	1	*Firmicutes, Bacilli*
Ochrobactrum sp. Ak1	1	*Alphaproteobacteria*
Stenotrophomonas sp. AMS3	1	*Gammaproteobacteria*
Stenotrophomonas sp. M2	1	*Gammaproteobacteria*
Total clone number	50	

Anolytic bacterial communities in the LR-MFC at day 564		
Mostly related microorganism	Number of clone	Phylogenetic phylum
Rhodopseudomonas palustris	16	*Alphaproteobacteria*
Azonexus caeni gene	14	*Betaproteobacteria*
Anaerovibrio burkinabensis DSM 6283(T)	7	*Firmicutes, Negativicutes*
Geobacter sp. LAR-2	4	*Deltaproteobacteria*
Thauera linaloolentis gene	4	*Betaproteobacteria*
Azoarcus sp. GPTSA12	2	*Betaproteobacteria*
Rhodobacter sphaeroides strain S6-1-1	2	*Alphaproteobacteria*
Rhodopseudomonas sp. S8-1	2	*Alphaproteobacteria*
Veillonellaceae bacterium 6-15 gene	2	*Firmicutes, Negativicutes*
Acetobacterium sp. HAAP-1	1	*Firmicutes, Clostridia*
Acetobacterium submarinus	1	*Firmicutes, Clostridia*
Phenylobacterium falsum partial	1	*Alphaproteobacteria*
Rhodobacter sphaeroides strain S10-1	1	*Alphaproteobacteria*
Rumen bacterium R-7	1	*Bacteria*
Thauera sp. Dec07-TCBS-7BB-c-3	1	*Betaproteobacteria*
Thiobacillus thioparus strain Pankhurst T4	1	*Betaproteobacteria*
Xanthomonadaceae bacterium NML 93-0792	1	*Gammaproteobacteria*
Xanthomonas sp. AF11	1	*Gammaproteobacteria*
Total clone number	62	

Anolytic bacterial communities in the HR-MFC at day 197		
Mostly related microorganism	Number of clone	Phylogenetic phylum
Clostridium sp. 6-44	5	*Firmicutes, Clostridia*
Clostridiales bacterium JN18_A56_K	3	*Firmicutes, Clostridia*
Synergistetes bacterium 7WAY-8-7	3	*Bacteria, Synergistetes.*
Acidaminococcus sp. BV3L6	2	*Firmicutes, Negativicutes*
Anaerovibrio burkinabensis DSM 6283(T)	2	*Firmicutes, Negativicutes*
Desulfovibrio desulfuricans strain ATCC 27774	2	*Deltaproteobacteria*
Hydrogenophaga bisanensis strain K102	2	*Betaproteobacteria*
Klebsiella oxytoca clone C06	2	*Gammaproteobacteria*
Ochrobactrum anthropi strain SL2	2	*Alphaproteobacteria*
Rhizobium sp. R-24658	2	*Alphaproteobacteria*
Thauera linaloolentis	2	*Betaproteobacteria*
Acetobacterium sp. HAAP-1	1	*Firmicutes, Clostridia*
Acetobacterium submarinus	1	*Firmicutes, Clostridia*
Achromobacter sp. BG105	1	*Betaproteobacteria*
Alpha proteobacterium PI_GH2.1.D7	1	*Alphaproteobacteria*
Bacterium S2342	1	*Bacteria*
Clostridium botulinum F str. 230613	1	*Firmicutes, Clostridia*
Mesorhizobium sp. Jip01	1	*Alphaproteobacteria*
Methyloversatilis sp. 3t	1	*Betaproteobacteria*
Proteobacterium K2	1	*Bacteria*
Rhodobacter sphaeroides strain S6-1-1	1	*Alphaproteobacteria*
Stenotrophomonas acidaminiphila	1	*Gammaproteobacteria*
Thermomonas haemolytica isolate TJ7	1	*Gammaproteobacteria*
Total clone number	39	

Continued supplemental material Table S2

Anolytic bacterial communities in the HR-MFC at day 333		
Mostly related microorganism	Number of clone	Phylogenetic phylum
Thauera linaloolentis	29	*Betaproteobacteria*
Acetobacterium submarinus	3	*Firmicutes, Clostridia*
Geobacter sp. LAR-2	2	*Deltaproteobacteria*
Hydrogenophaga sp. AR20	2	*Betaproteobacteria*
Acetanaerobacterium elongatum strain Z7	1	*Firmicutes, Clostridia*
Acetobacterium sp. HAAP-1	1	*Firmicutes, Clostridia*
Acetobacterium sp. R6T	1	*Firmicutes, Clostridia*
Achromobacter xylosoxidans strain WB-24	1	*Betaproteobacteria*
Anaerobic bacterium sk.prop8	1	*Firmicutes, Clostridia*
Anaerovibrio burkinabensis DSM 6283(T)	1	*Firmicutes, Negativicutes*
Azoarcus sp. GPTSA12	1	*Betaproteobacteria*
Brevundimonas bullata strain 1A6	1	*Alphaproteobacteria*
Christensenella minuta	1	*Firmicutes, Clostridia*
Desulfomicrobium baculatum DSM 4028	1	*Deltaproteobacteria*
Endosymbiont of Acanthamoeba sp. AC305	1	*Bacteria*
Ochrobactrum anthropi	1	*Alphaproteobacteria*
Rhodobacter sphaeroides strain S10-1	1	*Alphaproteobacteria*
Rhodopseudomonas palustris	1	*Alphaproteobacteria*
Stenotrophomonas acidaminiphila strain st31	1	*Gammaproteobacteria*
Synergistetes bacterium 7WAY-8-7	1	*Bacteria, Synergistetes*
	52	

Anolytic bacterial communities in the HR-MFC at day 427		
Mostly related microorganism	Number of clone	Phylogenetic phylum
Rhodobacter sphaeroides strain S10-1	10	*Alphaproteobacteria*
Rhodopseudomonas palustris	9	*Alphaproteobacteria*
Brevundimonas sp. X60	7	*Alphaproteobacteria*
Alcaligenes faecalis subsp. parafaecalis strain ALK518	4	*Betaproteobacteria*
Bacterium KKCSSW	4	*Bacteria*
Alcaligenes faecalis strain BAB-1832	2	*Betaproteobacteria*
Alcaligenes faecalis subsp. faecalis strain SK12	2	*Betaproteobacteria*
Ochrobactrum anthropi partial	2	*Alphaproteobacteria*
Alcaligenes faecalis strain CD234	1	*Betaproteobacteria*
Alpha proteobacterium BAL284	1	*Alphaproteobacteria*
Brevundimonas sp. H208	1	*Alphaproteobacteria*
Brevundimonas sp. LC437	1	*Alphaproteobacteria*
Brevundimonas sp. S-SL-1	1	*Alphaproteobacteria*
Ochrobactrum anthropi strain W-7	1	*Alphaproteobacteria*
Ochrobactrum sp. DX2	1	*Alphaproteobacteria*
Ochrobactrum sp. JS-4	1	*Alphaproteobacteria*
Ochrobactrum sp. n-9	1	*Alphaproteobacteria*
Rhodopseudomonas palustris strain HZ-5	1	*Alphaproteobacteria*
Rhodopseudomonas sp. JA576 partial	1	*Alphaproteobacteria*
Rhodopseudomonas sp. S8-1	1	*Alphaproteobacteria*
Total clone number	52	

Anolytic bacterial communities in the HR-MFC at day 564		
Mostly related microorganism	Number of clone	Phylogenetic phylum
Azoarcus sp. GPTSA12	23	*Betaproteobacteria*
Thauera linaloolentis gene	14	*Betaproteobacteria*
Rhodopseudomonas palustris	11	*Alphaproteobacteria*
Acetobacterium submarinus	7	*Firmicutes, Clostridia*
Azonexus caeni gene	3	*Betaproteobacteria*
Bacterium ROMEm59sa320	2	*Bacteria*
Spirochaetes bacterium SA-10	2	*Bacteria, Spirochaetes*
Acetobacterium sp. HAAP-1	1	*Firmicutes, Clostridia*
Acetobacterium wieringae strain DP9	1	*Firmicutes, Clostridia*
Azovibrio sp. R-25062	1	*Betaproteobacteria*
Geobacter sp. LAR-2	1	*Deltaproteobacteria*
Hydrogenophaga sp. AR20 gene	1	*Betaproteobacteria*
Rhodobacter sphaeroides strain S10-1	1	*Alphaproteobacteria*
Rhodocyclaceae bacterium FTL11	1	*Betaproteobacteria*
Spirochaeta stenostrepta partial	1	*Bacteria, Spirochaetes*
Xanthomonadaceae bacterium NML 93-0792	1	*Gammaproteobacteria*
Xanthomonas sp. AF11	1	*Gammaproteobacteria*
Total clone number	72	

Continued supplemental material Table S2

Biofilm communities in the LR-MFC at day 197		
Mostly related microorganism	Number of clone	Phylogenetic phylum
Geobacter sp. LAR-2	10	*Deltaproteobacteria*
Rhodopseudomonas palustris	9	*Alphaproteobacteria*
Anaerovibrio burkinabensis DSM 6283(T)	7	*Firmicutes, Negativicutes*
Ochrobactrum anthropi	5	*Alphaproteobacteria*
Thauera linaloolentis	3	*Betaproteobacteria*
Acetobacterium sp. HAAP-1	2	*Firmicutes, Clostridia*
Clostridium sp. SW001	2	*Firmicutes, Clostridia*
Pseudomonas brenneri strain G10	2	*Gammaproteobacteria*
Rhodobacter sphaeroides strain S10-1	2	*Alphaproteobacteria*
Rhodocyclaceae bacterium FTL11	2	*Betaproteobacteria*
Bacterium CBIC45I	1	*Bacteria*
Carnobacteriaceae bacterium FH025	1	*Firmicutes, Bacilli*
Clostridium sp. 6-44	1	*Firmicutes, Clostridia*
Clostridium sticklandii str. DSM 519 chromosome	1	*Firmicutes, Clostridia*
Desulfovibrio vulgaris strain I5	1	*Deltaproteobacteria*
Rhodobacter sphaeroides strain S6-1-1	1	*Alphaproteobacteria*
Unidentified eubacterium from anoxic bulk soil	1	*Bacteria*
Xanthobacter agilis	1	*Alphaproteobacteria*
Total clone number	52	

Biofilm communities in the LR-MFC at day 333		
Mostly related microorganism	Number of clone	Phylogenetic phylum
Anaerovibrio burkinabensis DSM 6283(T)	14	*Firmicutes, Negativicutes*
Geobacter sp. LAR-2	4	*Deltaproteobacteria*
Rhodopseudomonas palustris	4	*Alphaproteobacteria*
Acetobacterium wieringae strain DP9	3	*Firmicutes, Clostridia*
Clostridium favososporum partial	3	*Firmicutes, Clostridia*
Clostridium sp. SW001	3	*Firmicutes, Clostridia*
Acetobacterium submarinus	2	*Firmicutes, Clostridia*
Acholeplasma sp. DM-2009 strain Lorelei	1	*Bacteria, Tenericutes*
Azonexus caeni gene	1	*Betaproteobacteria*
Azospirillum sp. TS15	1	*Alphaproteobacteria*
Clostridium sp. PPf35E6	1	*Firmicutes, Clostridia*
Clostridium sticklandii str. DSM 519 chromosome	1	*Firmicutes, Clostridia*
Desulfomicrobium baculatum DSM 4028	1	*Deltaproteobacteria*
Desulfovibrio sp. A1	1	*Deltaproteobacteria*
Ochrobactrum sp. OTU29	1	*Alphaproteobacteria*
Rhodopseudomonas sp. JA772 partial	1	*Alphaproteobacteria*
Spirochaetes bacterium SA-10	1	*Bacteria, Spirochaetes*
Thauera linaloolentis gene	1	*Betaproteobacteria*
Total clone number	44	

Biofilm communities in the LR-MFC at day 427		
Mostly related microorganism	Number of clone	Phylogenetic phylum
Acetobacterium sp. HAAP-1	7	*Firmicutes, Clostridia*
Azoarcus sp. GPTSA12	6	*Betaproteobacteria*
Azonexus caeni gene	5	*Betaproteobacteria*
Thauera linaloolentis	5	*Betaproteobacteria*
Anaerovibrio burkinabensis DSM 6283(T)	4	*Firmicutes, Negativicutes*
Acetobacterium submarinus	2	*Firmicutes, Clostridia*
Bacterium ROME195Asa	2	*Bacteria*
Geobacter sp. SD-1	2	*Deltaproteobacteria*
Veillonellaceae bacterium 6-15	2	*Firmicutes, Negativicutes*
Acetobacterium wieringae strain DP9	1	*Firmicutes, Clostridia*
Acidaminococcus sp. BV3L6	1	*Firmicutes, Negativicutes*
Acidobacteria bacterium KBS 96	1	*Bacteria, Acidobacteria*
Alpha proteobacterium PI_GH2.1.D7	1	*Alphaproteobacteria*
Bacillus sp. IST-38 partial	1	*Firmicutes, Bacilli*
Bacterium ROMEm59sa320	1	*Bacteria.*
Clostridium favososporum partial	1	*Firmicutes, Clostridia*
Clostridium sp. MH18	1	*Firmicutes, Clostridia*
Ensifer sp. 8_88 partial	1	*Alphaproteobacteria*
Geobacter sp. LAR-2	1	*Deltaproteobacteria*
Methyloversatilis sp. 3t	1	*Betaproteobacteria*
Rhodobacter sphaeroides strain S10-1	1	*Alphaproteobacteria*
Rhodocyclaceae bacterium FTL11	1	*Betaproteobacteria*
Rhodopseudomonas palustris	1	*Alphaproteobacteria*
Unidentified eubacterium from anoxic bulk soil	1	*Bacteria*
Total clone number	50	

Continued supplemental material Table S2

Biofilm communities in the LR-MFC at day 564		
Mostly related microorganism	Number of clone	Phylogenetic phylum
Novosphingobium sediminicola strain HU1-AH51	12	*Alphaproteobacteria*
Geobacter sp. LAR-2	11	*Deltaproteobacteria*
Anaerovibrio burkinabensis DSM 6283(T)	8	*Firmicutes, Negativicutes*
Burkholderia sp. A39	4	*Betaproteobacteria*
Rhodopseudomonas palustris	3	*Alphaproteobacteria*
Burkholderia cepacia partial	2	*Betaproteobacteria*
Geobacter sp. SD-1	2	*Deltaproteobacteria*
Acholeplasma sp. DM-2009 strain Lorelei	1	*Bacteria, Tenericutes*
Bacterium 11RO2	1	*Bacteria*
Burkholderia cepacia isolate 4	1	*Betaproteobacteria*
Burkholderia sp. A45	1	*Betaproteobacteria*
Burkholderia sp. SR2-07	1	*Betaproteobacteria*
Burkholderia sp. TCP30	1	*Betaproteobacteria*
Caulobacter sp. 44	1	*Alphaproteobacteria*
Desulfovibrio desulfuricans strain ATCC 27774	1	*Deltaproteobacteria*
Ochrobactrum anthropi strain X-12	1	*Alphaproteobacteria*
Rhizobium borbori strain DN365	1	*Alphaproteobacteria*
Rhodobacter sphaeroides strain S10-1	1	*Alphaproteobacteria*
Rhodopseudomonas sp. S8-1	1	*Alphaproteobacteria*
Sphingomonas sp. 070605-23_L09_7	1	*Alphaproteobacteria*
Sphingomonas sp. strain B28161	1	*Alphaproteobacteria*
Sporomusa sp. DR15	1	*Firmicutes, Negativicutes*
Thauera linaloolentis gene	1	*Betaproteobacteria*
Trichococcus sp. N1	1	*Firmicutes, Bacilli*
Unidentified eubacterium from anoxic bulk soil	1	*Bacteria*
Veillonellaceae bacterium 6-15 gene	1	*Firmicutes, Negativicutes*
Total clone number	61	

Biofilm communities in the HR-MFC at day 197		
Mostly related microorganism	Number of clone	Phylogenetic phylum
Acetobacterium submarinus	10	*Firmicutes, Clostridia*
Geobacter sp. SD-1	9	*Deltaproteobacteria*
Geobacter sp. LAR-2	7	*Deltaproteobacteria*
Anaerovibrio burkinabensis DSM 6283(T)	6	*Firmicutes, Negativicutes*
Azoarcus sp. GPTSA12	4	*Betaproteobacteria*
Rhodopseudomonas palustris	3	*Alphaproteobacteria*
Azospirillum sp. TS18 gene	2	*Alphaproteobacteria*
Desulfovibrio sp. ds3	2	*Deltaproteobacteria*
Azonexus fungiphilus partial	1	*Betaproteobacteria*
Bacterium ROMEm59sa320	1	*Bacteria*
Christensenella minuta	1	*Firmicutes, Clostridia*
Comamonas sp. CHb	1	*Betaproteobacteria*
Cytophaga xylanolytica	1	*Bacteria, Bacteroidetes*
Desulfovibrio vulgaris subsp. vulgaris str. Hildenborough	1	*Deltaproteobacteria*
Escherichia coli strain 6	1	*Gammaproteobacteria*
Geobacter sulfurreducens PCA	1	*Deltaproteobacteria*
Ochrobactrum anthropi partial	1	*Alphaproteobacteria*
Ochrobactrum sp. DX2	1	*Alphaproteobacteria*
Propionibacterium freudenreichii strain ISU P59	1	*Bacteria, Actinobacteria*
Rhodobacter sp. Bo10-19	1	*Alphaproteobacteria*
Rhodobacter sphaeroides strain S10-1	1	*Alphaproteobacteria*
Rumen bacterium R-7	1	*Bacteria*
Spirochaetes bacterium SA-10	1	*Bacteria, Spirochaetes*
Total clone number	58	

Biofilm communities in the HR-MFC at day 333		
Mostly related microorganism	Number of clone	Phylogenetic phylum
Thauera linaloolentis	17	*Betaproteobacteria*
Acetobacterium sp. HAAP-1	5	*Firmicutes, Clostridia*
Desulfomicrobium baculatum DSM 4028	5	*Deltaproteobacteria*
Geobacter sp. LAR-2	5	*Deltaproteobacteria*
Acetobacterium submarinus	4	*Firmicutes, Clostridia*
Spirochaetes bacterium SA-10	3	*Bacteria, Spirochaetes*
Thauera linaloolentis gene	3	*Betaproteobacteria*
Acetobacterium wieringae strain DP9	2	*Firmicutes, Clostridia*
Desulfovibrio vulgaris str. 'Miyazaki F'	2	*Deltaproteobacteria*
Geobacter sp. SD-1	2	*Deltaproteobacteria*
Azoarcus sp. GPTSA12	1	*Betaproteobacteria*
Christensenella minuta	1	*Firmicutes, Clostridia*
Desulfovibrio termitidis	1	*Deltaproteobacteria*
Laribacter hongkongensis HLHK9	1	*Betaproteobacteria*
Pelotomaculum propionicicum gene	1	*Firmicutes, Clostridia*
Rhodobacter sphaeroides strain S10-1	1	*Alphaproteobacteria*
Rhodopseudomonas palustris	1	*Alphaproteobacteria*
Synergistetes bacterium 7WAY-8-7	1	*Bacteria, Synergistetes*
Thauera sp. Dec07-TCBS-7BB-c-3	1	*Betaproteobacteria*
Unidentified eubacterium from anoxic bulk soil	1	*Bacteria*
Total clone number	58	

Continued supplemental material Table S2

Biofilm communities in the HR-MFC at day 427		
Mostly related microorganism	Number of clone	Phylogenetic phylum
Acetobacterium sp. HAAP-1	19	*Firmicutes, Clostridia*
Christensenella minuta	4	*Betaproteobacteria*
Thauera linaloolentis	4	*Betaproteobacteria*
Azoarcus sp. GPTSA12	2	*Betaproteobacteria*
Clostridium cellobioparum	2	*Firmicutes, Clostridia*
Clostridium sp. YMB55	2	*Firmicutes, Clostridia*
Papillibacter cinnaminovorans	2	*Firmicutes, Clostridia*
Rhodopseudomonas palustris	2	*Alphaproteobacteria*
Acetanaerobacterium elongatum strain Z7	1	*Firmicutes, Clostridia*
Acidovorax sp. XJ-2	1	*Betaproteobacteria*
Anaerovibrio burkinabensis DSM 6283(T)	1	*Firmicutes, Negativicutes*
Bacterium ROMEm59sa320	1	*Bacteria*
Bacterium S2321	1	*Bacteria*
Bacterium WH6-7	1	*Bacteria*
Gracilibacter thermotolerans strain JW/YJL-S clone 5	1	*Firmicutes, Clostridia*
Paenibacillus sp. MM38	1	*Firmicutes, Bacilli*
Pelotomaculum propionicicum	1	*Firmicutes, Clostridia*
Rumen bacterium R-7	1	*Bacteria*
Spirochaeta stenostrepta partial	1	*Bacteria, Spirochaetes*
Synergistetes bacterium 7WAY-8-7	1	*Bacteria, Synergistetes.*
Unidentified eubacterium from anoxic bulk soil	1	*Bacteria*
Total clone number	50	

Biofilm communities in the HR-MFC at day 564		
Mostly related microorganism	Number of clone	Phylogenetic phylum
Acetobacterium submarinus	20	*Firmicutes, Clostridia*
Azoarcus sp. GPTSA12	6	*Betaproteobacteria*
Geobacter sp. LAR-2	6	*Deltaproteobacteria*
Rhodopseudomonas palustris	6	*Alphaproteobacteria*
Bacterium ROMEm59sa320	5	*Bacteria*
Thauera linaloolentis gene	4	*Betaproteobacteria*
Anaerovibrio burkinabensis DSM 6283(T)	2	*Firmicutes, Negativicutes*
Azonexus caeni gene	2	*Betaproteobacteria*
Geobacter sp. SD-1	2	*Deltaproteobacteria*
Spirochaetes bacterium SA-10	2	*Bacteria, Spirochaetes*
Acetobacterium sp. HAAP-1	1	*Firmicutes, Clostridia*
Acidaminococcus sp. BV3L6	1	*Firmicutes, Negativicutes*
Dehalobacterium formicoaceticum	1	*Firmicutes, Bacilli*
Holosporaceae bacterium Serialkilleuse_9403403	1	*Alphaproteobacteria*
Hydrogenophaga sp. AR20 gene	1	*Betaproteobacteria*
Lachnospiraceae bacterium 19gly4	1	*Firmicutes, Clostridia*
Pelotomaculum propionicicum gene	1	*Firmicutes, Clostridia*
Rhodobacter sp. Bo10-19	1	*Alphaproteobacteria*
Rhodocyclaceae bacterium FTL11	1	*Betaproteobacteria*
Rhodopseudomonas sp. S8-1	1	*Alphaproteobacteria*
Thiobacillus thioparus strain Pankhurst T4	1	*Betaproteobacteria*
Total clone number	66	

Supplementary material figure legends

Fig. S1. Schematic diagram of the MFC used in this study.
1: outer plate, 2: inner silicone rubber plate, 3: cathode, 4: Nafion membrane, 5: inner plate, 6: inner silicone rubber frame, 7: the main body, 8: outer plate without window.

Fig. S2. Schematic diagram of $E^{0'}_{anode}$, and onset potential.
(A) Explanation of $E^{0'}_{anode}$, and onset potential, (B) The onset potential is defined as most negative potential in the Tafel plot. A Tafel plot shows the exponential phase in potential (V) vs. log (current density) shown as the gray dashed line.

Fig. S3. DGGE profiles of partial 16S rRNA gene fragments.
(A) and (B) from the LR-MFC, (C) and (D) from the HR-MFC. (E) Compensation of the intensity and position of DGGE bands between the LR-MFC and HR-MFC. Numbers noted above the photograph indicate sampling days. "B" means that the samples were biofilms communities attached on the anode surface.

Fig. S4. The program of MDS analysis on R used in this study.
The program shown here is one of some programs for MDS analysis. "File name.txt" is a matrix data which consists of intensities and locations of DGGE bands.

Fig. S5. A phylogenetic tree based on partial 16S rRNA gene sequences of representative *Geobacter* isolates and *Geobacteraceae* sequence phylotypes retrieved in this study (indicated by bold letters). The number indicates the sampling date. "L" and "H" above the number denote the LR-MFC and the HR-MFC, respectively. "A" and "B" next to the number indicates anolytic and biofilm samples, respectively. "Sediment" means the inoculum sample. The numbers of clones retrieved from different libraries are shown in square brackets. The novel *Geobacter* clade was reported in a previous study (1). Only bootstrap values >500 are shown. The bar represents 0.01 substitutions per site.

Fig. S6. Gel image of electrophoresis using *Geobacter* specific primer. M: marker, A, B, and C: clone closely related to *Geobacter metallireducence* clade, G: *Geobacter sulfurreducens*, N: negative control. White arrow indicates the purpose amplified DNA fragment using set of primers New *Geo*-f and New *Geo*-r.

Fig. S7. Monitoring of organic acids in effluents from MFCs.
(A): LR-MFC, and (B): HR-MFC. Arrows mean the addition of lactate in MFCs. Black bar means that the sampling was not conducted.

Fig. S8. Chronopotentiometry analyses data of LR-MFC (A) and HR-MFC (B).
Closed symbols indicate the data from anode. Open symbols indicate the data from cathode. Red diamond, day 156; red square, day 258; yellow triangle, day 366; green circular, day 400; green diamond, day 429; blue square, day 478; blue triangle, day 521; and purple circular, day 568.

Fig. S9. Low-san cyclic voltammograms of LR-MFC (A-H) and HR-MFC (I-P). The voltammogram was recorded at a scan rate of 1 mV s^{-1}. Black and gray lines represent the data of first and second circular, respectively. A and I, day 198; B and J, day 216; C and K, day 257; D and L, day 312; E and M, day 364; F and N, day 399; G and O, day 491; H and P, day 576.

Reference of supplementary material figures

1. **Yamamoto, S., Suzuki, K., Araki, Y., Mochihara, H., Hosokawa, T., Kubota, H., Chiba, Y., Rubaba, O., Tashiro, Y., and Futamata. H.:** Dynamics of different bacterial communities are capable of generating sustainable electricity from microbial fuel cell with organic waste, Microbes Environ., **29,** 145-153 (2014).